1944

Ferro-inductance as a variable electric circuit element

John Douglas Ryder
Iowa State College

FERRO-INDUCTANCE AS A VARIABLE ELECTRIC CIRCUIT ELEMENT

by

John Douglas Ryder

A Thesis Submitted to the Graduate Faculty
for the Degree of

DOCTOR OF PHILOSOPHY

Major Subject: Electrical Engineering

Approved:

Signature was redacted for privacy.

In Charge of Major Work

Signature was redacted for privacy.

Head of Major Department

Signature was redacted for privacy.

Dean of Graduate College

Iowa State College

1944

TABLE OF CONTENTS

I. Introduction

A. Ferro-inductance as a Circuit Element

The introduction of the alternating current distribution system by George Westinghouse in 1885 and the development of the transformer by Stanley led to an early awareness of the properties of coils mounted on iron cores, or ferro-reactors, and of their actions in alternating current circuits. It was known that the inductance of such coils was not constant, but varied with the value of current flowing, and that this was not a linear relation, owing to the shape of the magnetization curve of the iron used.

Mathematical analysis of such circuits leads to differential equations with variable coefficients which are almost impossible of solution. To overcome this barrier and to obtain usable results the engineer is accustomed to assume the inductance of the ferro-reactor as constant, thereby obtaining differential equations with constant coefficients and an easy mathematical solution for the circuit. This method then leads to the use of complex algebra in still further simplifying the analysis.

However, this analysis, in terms of complex algebra or differential equations, is based on an assumption which in certain problems cannot be supported. This assumption is that of constant inductance, or that the value of the inductance is not a function of current or time.

The increased application of saturable core reactors, ferro-resonant circuits, tuned circuits with ferro-reactors, and fundamental studies of contactors and relays, have shown the older methods of design and analysis based on the constant inductance assumption to be inadequate. The present work was undertaken to develop on an engineering basis, methods of reactor design and of analysis of circuits containing ferro-inductors, whose inductance is a function of the current flowing.

B. Definitions

Inductance is the proportionality factor between instantaneous induced voltage and the rate of change of current in an electric circuit. That is,

$$e = -L \frac{di}{dt}$$

is the defining relation for inductance giving

$$L = \frac{-e}{\frac{di}{dt}} \qquad (1)$$

as the basic equation for inductance.

Rader and Litscher[14] have indicated a number of other definitions based on use or method of measurement. Many of these definitions are merely time averages of inductance weighted in various ways to produce certain desired results.

If it is remembered that equation (1) is a relationship between instantaneous quantities, then (1) becomes the fundamental defining relationship for inductance, and the other types summarized by Rader and Litscher become only special cases.

Ferro-inductance is a term used to designate the special properties of an inductance when iron is introduced into the magnetic circuit. Defining relation (1) still holds, but the value of L, the proportionality factor, is no longer a constant but is a function of i, the current.

Ferro-inductor or ferro-reactor are terms used as nouns to indicate coils with iron cores, having the properties of ferro-inductance.

C. Review of Literature

1. Non-linear characteristics of ferro-inductors.

Apparently the earliest application of the non-linear voltage-current characteristics of ferro-inductors was made by Zenneck[24] in 1899. This involved the use of transformers, with d-c excitation to accentuate the non-linearity, so connected as to produce doubling of the input frequency. This method became of considerable importance for radio-frequency generation in 1915-20 and was further reported on by Zenneck[25] and Ryan[15] in 1920. With the advent of the triode vacuum tube it ceased to have practical importance although it has been revived occasionally for special purposes.

The first report on the phenomena present in R-L-C series circuits, in which the L was ferro-inductive, was made by Martienssen[12] in 1910. This is the type of circuit which we now call ferro-resonant. Starting with circuit differential equations and considering the eddy current losses he was able to arrive at solutions for the resistance and inductance of the reactor, and from these solutions, to predict the shape of current-voltage relations to be expected in ferro-resonant circuits. However, it appears that in integrating the differential equations of the circuit, Martienssen treated μ of the iron as a constant, then later in his analysis allowed it to become a variable, thereby invalidating his results.

Apparently the ferro-resonant circuit with its interesting properties of multi-valued currents was not further investigated until about 1925 when some work was done in France. In 1931 Suits[17] published an important American paper on the subject, giving operating results, without attempt to develop methods of analysis, and suggesting several applications. In another paper[18] he reported on an application to a sharply selective voltage sensitive bridge and its uses in relay work.

Following the opening of the field of ferro-resonance by Suits, many other investigators gave it their attention. Boyajian[3] was the first to publish an analysis of the non-linear circuit action, basing his work on approximating the magnetization curve by two straight lines. Odessy and Weber[13] in 1938 developed a graphical method of determining the critical conditions in ferro-resonant circuits, but this was usable only with a previously determined voltage-current curve for the reactor, and does not aid in the design of the reactors.

Thomson[20,21,22] in 1938 and 1939 published a series of papers on ferro-resonant circuits but started with the measured reactance curves of a reactor. Thomson, and Odessy and Weber, thus did not provide a fundamental design analysis or circuit analysis. Their methods were usable only after a reactor had been built and could be measured, but gave no data on means by which a reactor could be designed and built to fulfill predetermined specifications. Keller[9] presented a mathematical solution of the ferro-resonant circuit differential equations. It is not well suited to general engineering design and calculation.

In considering the design of ordinary reactors and choke coils, a statement from the Bell Laboratories Record[23] that such coils cannot be designed, but must be measured under actual operating conditions, and a statement by Hanna[7] that the inductance of choke coils should be measured with a small a-c voltage, are typical of the lack of precision and the general disorder of this field.

It is easily seen that much fundamental work is needed in the development of methods of designing ferro-reactors to specifications, and of the analysis of circuits using such reactors.

2. Empirical equations for the magnetization curve.

Since the time the first magnetization curve was measured for a steel, there have been attempts to develop equations to fit the curve. These attempts have followed two paths of attack: (1) to find an empirical mathematical relation which fits the curve by mathematical methods only, or (2) to find such a relation by consideration of the physics of magnetization. It cannot be said that either method has been more successful than the other.

One of the oldest, and certainly the most famous, of the equations developed for the purpose is Frölich's equation. This usually gives a satisfactory fit up to approximately the knee of the magnetization curve and is of the form:

$$B = \frac{H}{a + bH} \qquad (2)$$

This is the equation of a displaced hyperbola, and provides two arbitrary constants, a and b.

Zenneck[25], in his 1920 paper on the analysis of magnetic frequency doublers, used the relation:

$$B = sH - s'H^3 \qquad (3)$$

with s and s^1 arbitrary constants. It should be noted that this equation cannot be used much beyond the knee of the magnetization curve because of the negative cubic term which causes the curve to fall beyond that point. Zenneck succeeded in obtaining an expression for the inductance of a ferro-inductor in terms of current and the arbitrary constants, but since this was incidental to the main point of his paper, he did not carry the matter further and presented no experimental proof of any of his work.

Ryan[15], also for analysis of magnetic frequency doublers, used the relation:

$$B = A \tan^{-1} ax + Cx \tag{4}$$

Noting that the series for $\tan^{-1} ax$ is

$$\tan^{-1} ax = ax - \frac{a^3 x^3}{3} + \frac{a^5 x^5}{5} - \frac{a^7 x^7}{7} + \text{------},$$

it can be seen that Zenneck used the first two terms of the series, and Ryan is a little more accurate in the use of the full series. Ryan does avoid the limitation at the knee of the curve which is forced upon Zenneck by the use of only the first two terms. Keller[9] used a series similar to the above.

Boyajian[3], in order to simplify the mathematics, used an approximation to the magnetization curve consisting of two straight lines, one for use below the knee, the other above. The results, while easily obtained, are not satisfactory for a quantitative design basis.

In 1926, Gokhale[5], using physical methods, developed the relation:

$$\beta = S\left(1 - b\varepsilon^{-aH}\right)$$

$$\beta = B - H \tag{5}$$

The saturation value of the steel is S, and $\mathcal{B}$ is the intrinsic induction. This equation is considerably limited in scope, giving a good fit to actual steel curves only in regions above the knee.

Rader and Litscher[14] have used the equation:

$$H = K_1 B + K_2 B^{10} \tag{6}$$

and while this fits the magnetization curves fairly well, it is impossible of use for circuit analysis, as will be discussed in the next section. Rader and Litscher used it to obtain values of ferro-inductance, but the results are obviously in error, since they indicate infinite values of inductance for zero current, whereas actual values of inductance are definitely finite.

II. A NEW EMPIRICAL EQUATION FOR THE MAGNETIZATION CURVE

A. Requirements to be Fulfilled

If an empirical relation for the magnetization curve is to be useful in the analysis of alternating current circuits it must be a function which behaves in every way exactly as the true magnetization curve. Since actual magnetization curves are "odd" functions, and display equal and opposite effects for positive and negative currents, then the function chosen to represent the magnetization curve must likewise be an "odd" function.

The magnetization curve affects our electric circuits only indirectly, through the phenomena of flux linkage changes or inductance. Since inductance is one of our basic circuit parameters, and since it appears frequently in circuit equations, it is obvious that for convenience alone, the equation chosen to represent the magnetization curve should lead to a simple expression for inductance.

If ease in circuit analysis is the aim, then the empirical relation for the magnetization curve should be chosen, first, to yield a simple inductance expression, and second, to fit the magnetization curve.

Since the defining relation has been chosen as:

$$e = -L \frac{di}{dt}$$

and since an induced emf may be expressed as:

$$e = -N \frac{d\phi}{dt} \times 10^{-8}$$

the two relations can be equated, giving:

$$L = N \frac{d\phi}{di} \times 10^{-8} \tag{7}$$

The magnetization curve is a plot of B against H, where B is proportional to ϕ and H to i; consequently $d\phi/di$ is the slope of the magnetization curve. Inductance is therefore proportional to the slope of the magnetization curve.

It is then possible to set up two criteria which a function, to be useful as an approximation to the magnetization curve of a steel, must filfill:

1. The function should be "odd".
2. The $d\phi/di$ of the function should be mathematically simple.

Applying this test to the functions used by other investigators it is seen that equations (3) and (4) of Zenneck and Ryan meet the first requirement above. The equations (5) of Gokhale, and (6) of Rader and Litscher, are entirely unsuited as they do not behave properly for negative values of the variable. Frolich's equation is also not suitable by this test.

The second requirement of the simple derivative is fulfilled by Zenneck's equation (3). The derivative of the $\tan^{-1}ax$ term of Ryan's equation (4) leads to a term of the form:

$$\frac{a}{a^2 + x^2}$$

where x involves the current. If the current is given by $I_m \sin\omega t$ then the fraction becomes:

$$\frac{a}{a^2 + K I_m^2 \sin^2 \omega t}$$

and the $\sin^2\omega t$ term can be written as a second harmonic. This expression, however, lacks physical significance.

This discussion has ruled out all the approximations considered except that of Zenneck:

$$B = sH - s'H^3 \qquad (3)$$

Equation (3), as was pointed out, is good only to the knee of the curve and is thereby seriously limited. Consequently none of the empirical relationships considered are suitable for the analysis of alternating current circuits. This would also apply to many other relationships which have been proposed from time to time. They have been developed wholly for the purpose of approximating the magnetization curve, without thought of using them for circuit analysis. Need for a new relationship to approximate the magnetization curve is seen.

B. The Gudermannian Function

One function which appears to be suitable as an odd function is tanh x. The derivative of tanh x is $\mathrm{sech}^2 x$ which is relatively simple and concise. Some work was done to approximate a magnetization curve with a function involving tanh x and fair agreement is usually easily obtained. An equation which has been used is:

$$B = s \tanh \frac{aNi}{l}$$

where S is the saturation value of the iron.

Work with the above equation led to the consideration of another function, the "gudermannian".[6] This function is defined as:

$$gd\ x = \tan^{-1}(\sinh x)$$

It is an odd function and has as its derivative sech x which is a simpler form than the derivative of tanh x. It therefore fulfills in satisfactory fashion the two requirements laid down for a function to define the magnetization curve, providing a satisfactory fit to curves for various steels can be obtained.

Curves of tanh x and gd x are plotted on Figure 1. The values of gd x are taken from the Smithsonian Tables[2] and are tabulated for certain intervals in appendix B. It can be seen that both these functions vary in the correct manner to fit a magnetization curve.

Various properties of the gudermannian are listed here since the subject is discussed in few texts:

$$gd\ 0 = 0 \qquad gd(+\infty) = \frac{\pi}{2}$$

$$gd(-x) = -gd\ x \qquad gd(-\infty) = -\frac{\pi}{2}$$

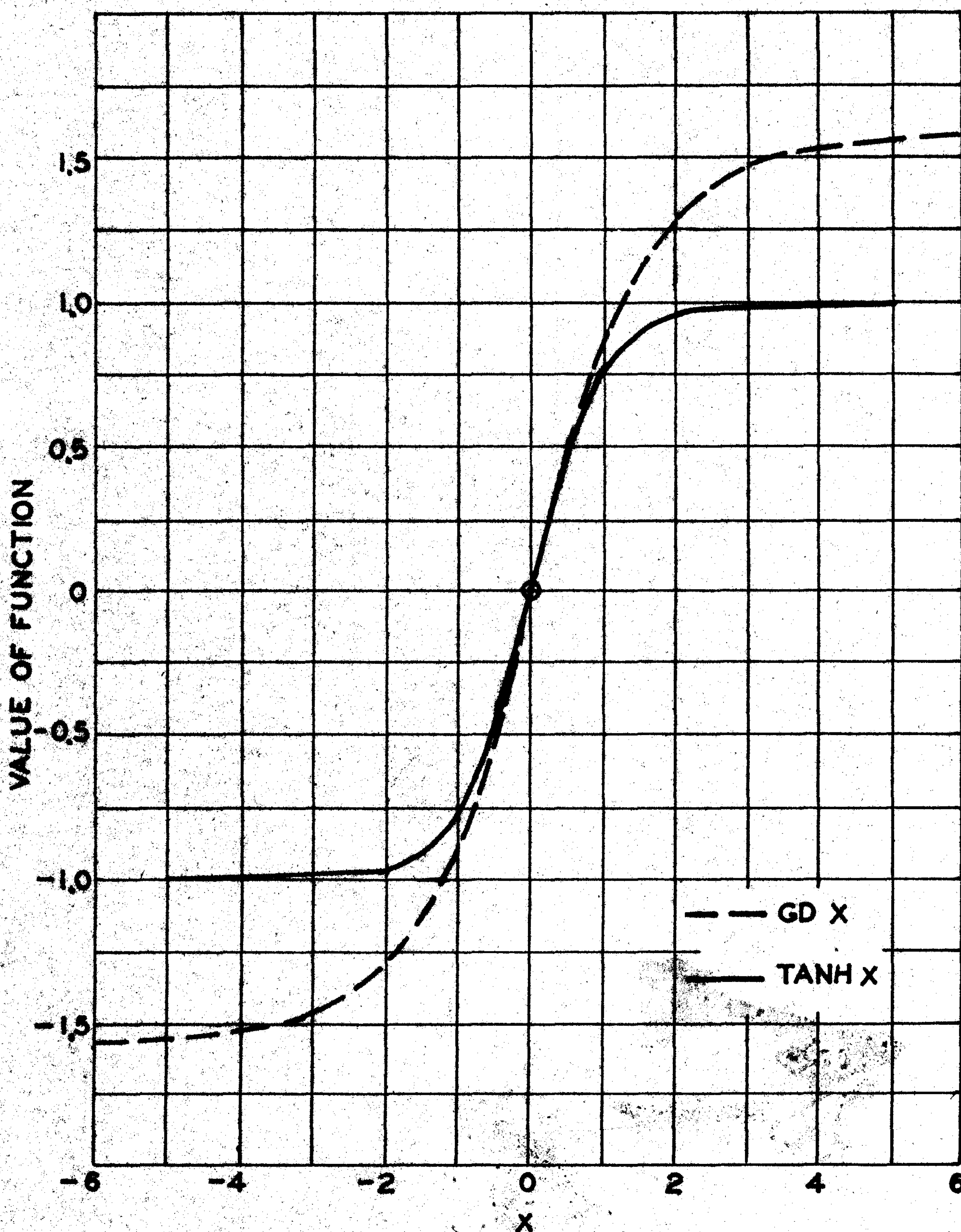

Fig. 1. Variation of tanh x and gd x.

From the definition of gd x:

$$\tan gd\,x = \sinh x$$

and since

$$\cosh^2 x = 1 + \sinh^2 x$$

it is possible to set up a right triangle:

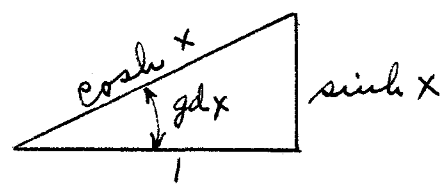

from which useful relationships between trigonometric and hyperbolic functions can be obtained. From the triangle can be seen:

$$\tan gd\,x = \sinh x$$
$$\sin gd\,x = \tanh x$$
$$\cos gd\,x = \operatorname{sech} x$$

These equations are useful properties of the gudermannian.

C. Fitting the Magnetization Curve

First attempts at curve fitting using the gudermannian in an expression of the form

$$B = B_n\, gd\, \frac{aNi}{l} \qquad (8)$$

were successful up to and somewhat above the knee at which point the gudermannian function saturated too rapidly. To help in this region a linear term was added to the relation, and since this resulted in three arbitrary constants over the previous two, a better overall fit was obtained for typical magnetization curves over very wide ranges. The empirical equation finally adopted was:

$$B = B_n \, gd \, \frac{aNi}{l} + \frac{cNi}{l} \quad (9)$$

It is interesting to note that this expression partakes considerably of the form of the well known relation:

$$B = \beta + H$$

where β is the intrinsic induction due to the steel and H is the induction due to the air alone. While the constant c is used to somewhat warp the gudermannian term and does not have the value to be expected if the cNi/l term were actually equivalent to H, yet the form of the equation is physically correct. The cNi/l term is usually small enough that it may be neglected frequently in analytic work.

Equation (9), being a transcendental relation, did not lend itself to easy direct solution for the values of the constants B_n, a, and c. The method developed was that of a trial process for a, after which B_n and c were obtained directly. This method is summarized as follows:

Select three points on the magnetization curve having coordinates x_1, y_1; x_2, y_2; x_3, y_3; where x is on the H axis and y on the B axis. The selection of these points is important if a good fit to the curve is to be obtained. Point x_1, y_1 should be chosen approximately at the point at which a line drawn from the origin with the greatest possible slope is tangent to the magnetization curve. Point x_2, y_2, should be chosen as somewhere near or above the middle of the curved portion of the knee and point x_3, y_3, at a position above the knee and having x_3 equal to $2x_2$ or greater.

It is possible, if x_3 or x_2 are chosen too low, to have c become a negative number and this is undesirable as the empirical curve will then droop at high values. The condition can be corrected by choosing larger values of x_3 or x_2.

Having chosen the desired points then the following equations may be written:

$$y_1 = B_n \, gd \, ax_1 + cx_1 \tag{10}$$

$$y_2 = B_n \, gd \, ax_2 + cx_2 \tag{11}$$

$$y_3 = B_n \, gd \, ax_3 + cx_3 \tag{12}$$

Multiply (10) by x_2, (11) by x_1;

$$x_2 y_1 = x_2 B_n \, gd \, ax_1 + cx_1 x_2$$

$$x_1 y_2 = x_1 B_n \, gd \, ax_2 + cx_1 x_2$$

Subtracting:

$$x_2 y_1 - x_1 y_2 = B_n \left[x_2 \, gd \, ax_1 - x_1 \, gd \, ax_2 \right] \tag{13}$$

Likewise multiply (11) by x_3 and (12) by x_2:

$$x_3 y_2 = x_3 B_n \, gd \, ax_2 + cx_2 x_3$$

$$x_2 y_3 = x_2 B_n \, gd \, ax_3 + cx_2 x_3$$

and after subtracting:

$$x_3 y_2 - x_2 y_3 = B_n \left[x_3 \, gd \, a x_2 - x_2 \, gd \, a x_3 \right] \tag{14}$$

Dividing (13) by (14):

$$\frac{x_2 y_1 - x_1 y_2}{x_3 y_2 - x_2 y_3} = \frac{x_2 \, gd \, a x_1 - x_1 \, gd \, a x_2}{x_3 \, gd \, a x_2 - x_2 \, gd \, a x_3}$$

$$(x_3 x_2 y_1 - x_3 x_1 y_2 + x_1 x_3 y_2 - x_1 x_2 y_3) \, gd \, a x_2$$
$$= x_2 (x_2 y_1 - x_1 y_2) \, gd \, a x_3 + x_2 (x_3 y_2 - x_2 y_3) \, gd \, a x_1$$

$$(x_3 y_1 - x_1 y_3) \, gd \, a x_2 = (x_2 y_1 - x_1 y_2) \, gd \, a x_3 + (x_3 y_2 - x_2 y_3) \, gd \, a x_1 \tag{15}$$

The coefficients of each term in equation (15) can be evaluated and the equation divided by the coefficient of the left hand term, resulting in:

$$gd \, a x_2 = F_1 \, gd \, a x_3 + F_2 \, gd \, a x_1 \tag{16}$$

Values of a are then assumed and inserted in (16) until the equation is satisfied, thereby fixing a for the particular steel being used. After determining a, its value may be inserted in (13) and (14) resulting in two values of B_n which should check. Either equations (10), (11) or (12) may then be used to obtain a value for c.

D. Results for Typical Steels

As an indication of the ability of equation (9) to approximate the magnetization curves for various commercial types of magnetic steels three types of steel were selected. The first, Westinghouse Hipersil, was selected as typical of modern high quality transformer steel. Since no magnetization curves were obtainable from the manufacturer the curve was measured in the laboratory. The second steel was Nicaloi (Allegheny 4750), a high nickel, high permeability alloy, typical of many high quality alloy steels. The magnetization curve was available from General Electric Company curve sheet H-4306424. The third steel chosen was common sheet steel, representative of the poorer quality steels occasionally used. This magnetization curve was also available from the General Electric Company curve sheet mentioned.

The equations determined for these three typical steels were:

Hipersil:

$$B = 65{,}000\, gd\left(0.273 \frac{Ni'}{l}\right) + 180 \frac{Ni'}{l} \tag{17}$$

Nicaloi:

$$B = 36{,}600\, gd\left(4.58 \frac{Ni'}{l}\right) + 6200 \frac{Ni'}{l} \tag{18}$$

Common sheet steel:

$$B = 51{,}800\, gd\left(0.087 \frac{Ni'}{l}\right) + 225 \frac{Ni'}{l} \tag{19}$$

Tables 1, 2 and 3 present the data for the magnetization curves using these equations, the curves being shown in Figures 2, 3 and 4. The measured curve or curve taken from manufacturer's data is shown solid, the curve computed from the equations is shown as a dashed line. Good agreement with the actual curves is shown for all three types of steel.

TABLE 1

Magnetization Data for Hipersil Steel

Ampere turns per inch	B measured Lines per inch^2	B calculated Equation (17)
2	30,000	34,100
4	59,500	60,700
6	79,500	77,200
8	90,000	89,000
10	95,400	95,400
12	98,500	99,300
15	101,400	102,600
20	104,300	105,200
30	107,400	107,500
40	108,300	109,300

TABLE 2

Magnetization Data for Nicaloi Steel

Ampere turns per inch	B Published data Lines per in^2	B Calculated Equation (18)
0.1	10,000	16,800
0.2	29,000	30,800
0.3	40,500	41,200
0.4	48,500	49,500
0.5	53,000	53,200
0.6	56,000	56,500
0.8	59,800	60,500
1.0	62,500	62,900
1.4	66,400	66,200
1.8	68,600	68,600
2.0	69,500	69,900

TABLE 3

Magnetization Data for Common Sheet Steel

Ampere turns per inch	B Published data Lines per $inch^2$	B Calculated Equation (19)
5	9,700	22,900
10	38,600	42,400
12	50,500	49,000
15	59,000	57,300
20	68,400	67,900
24	74,000	74,000
35	83,500	84,300
45	89,400	89,400
60	94,800	94,300
80	99,300	99,300

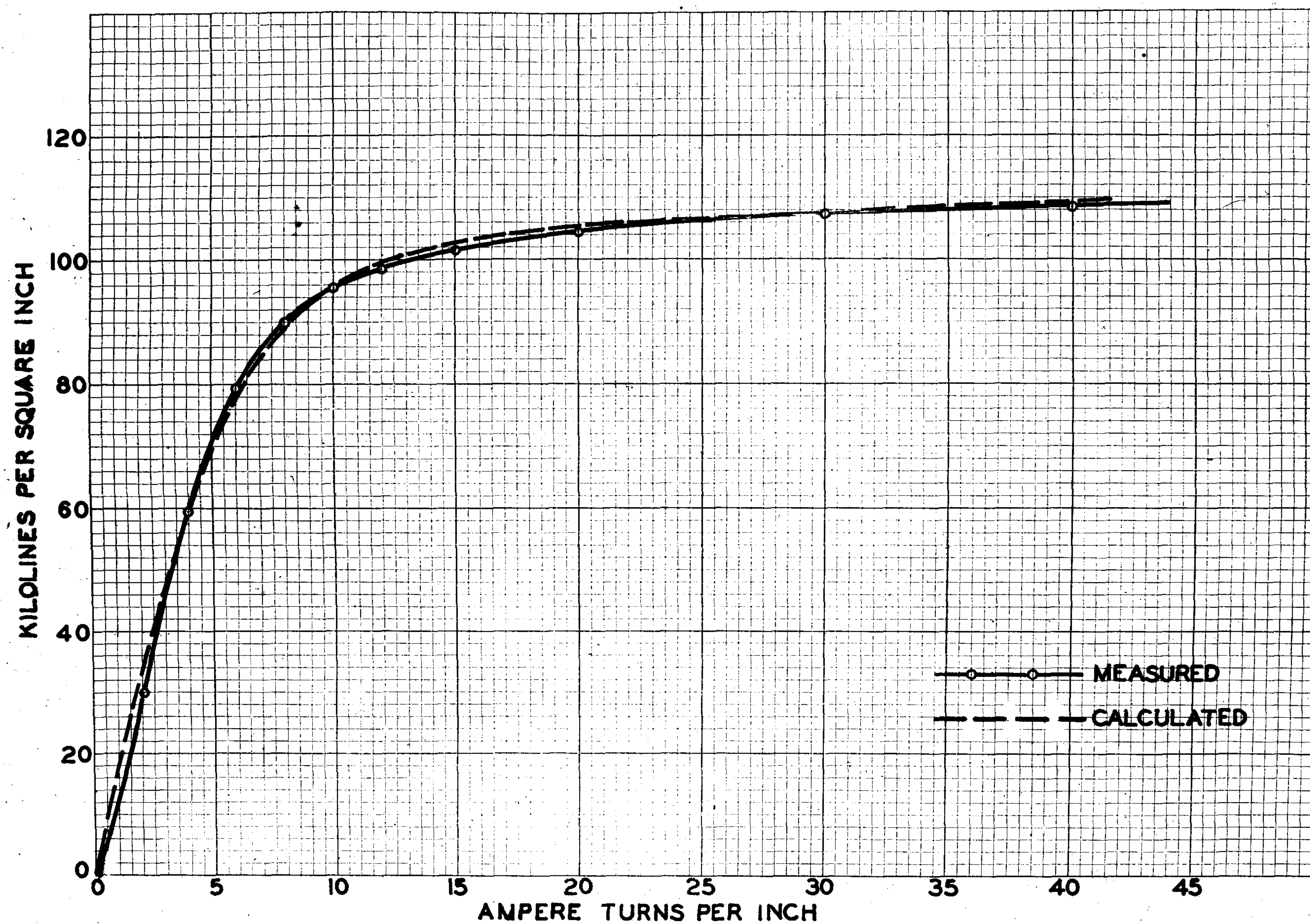

Fig. 2. Magnetization Curve for Hipersil Steel.

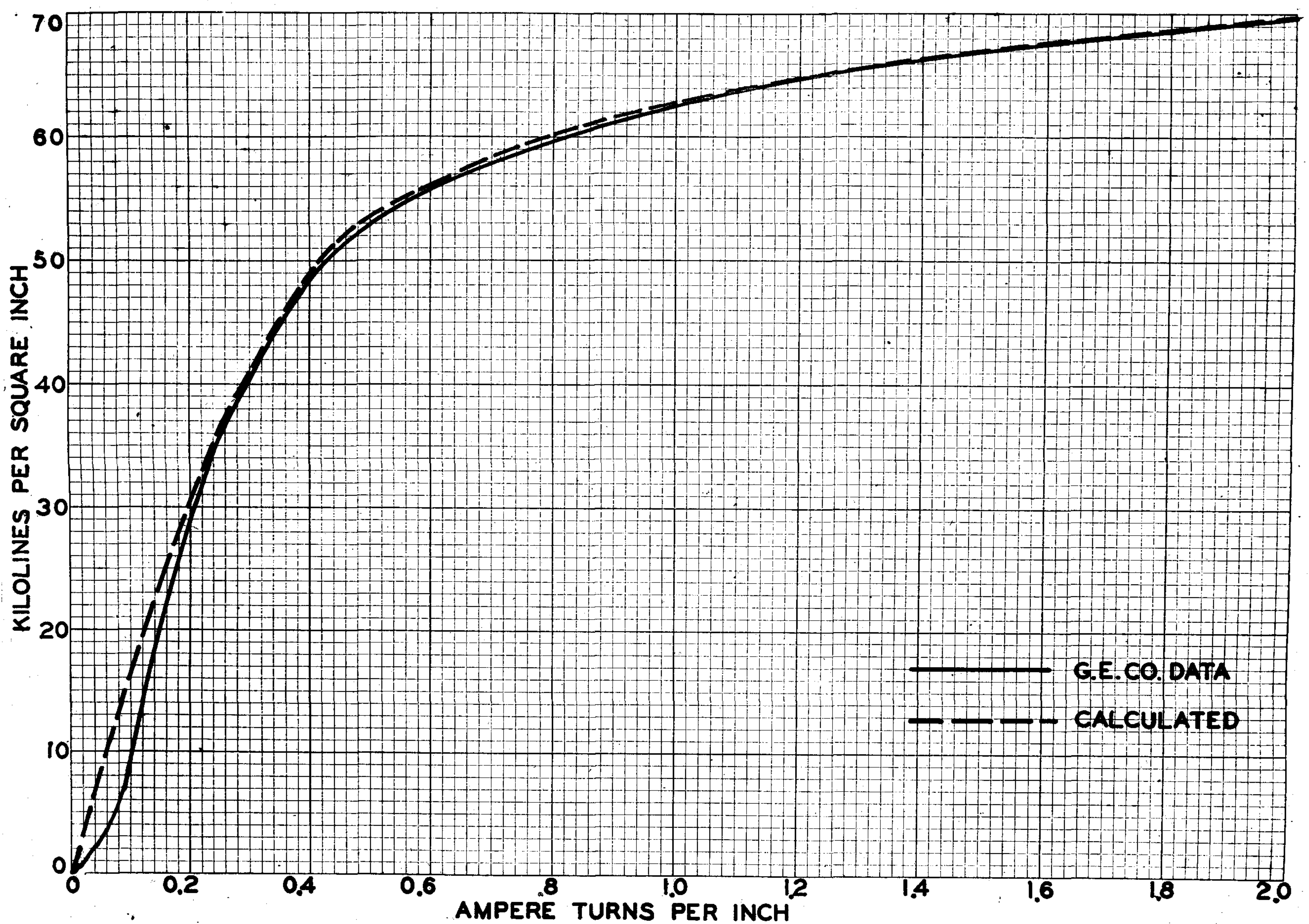

Fig. 3. Magnetization Curve for Nicaloi Steel.

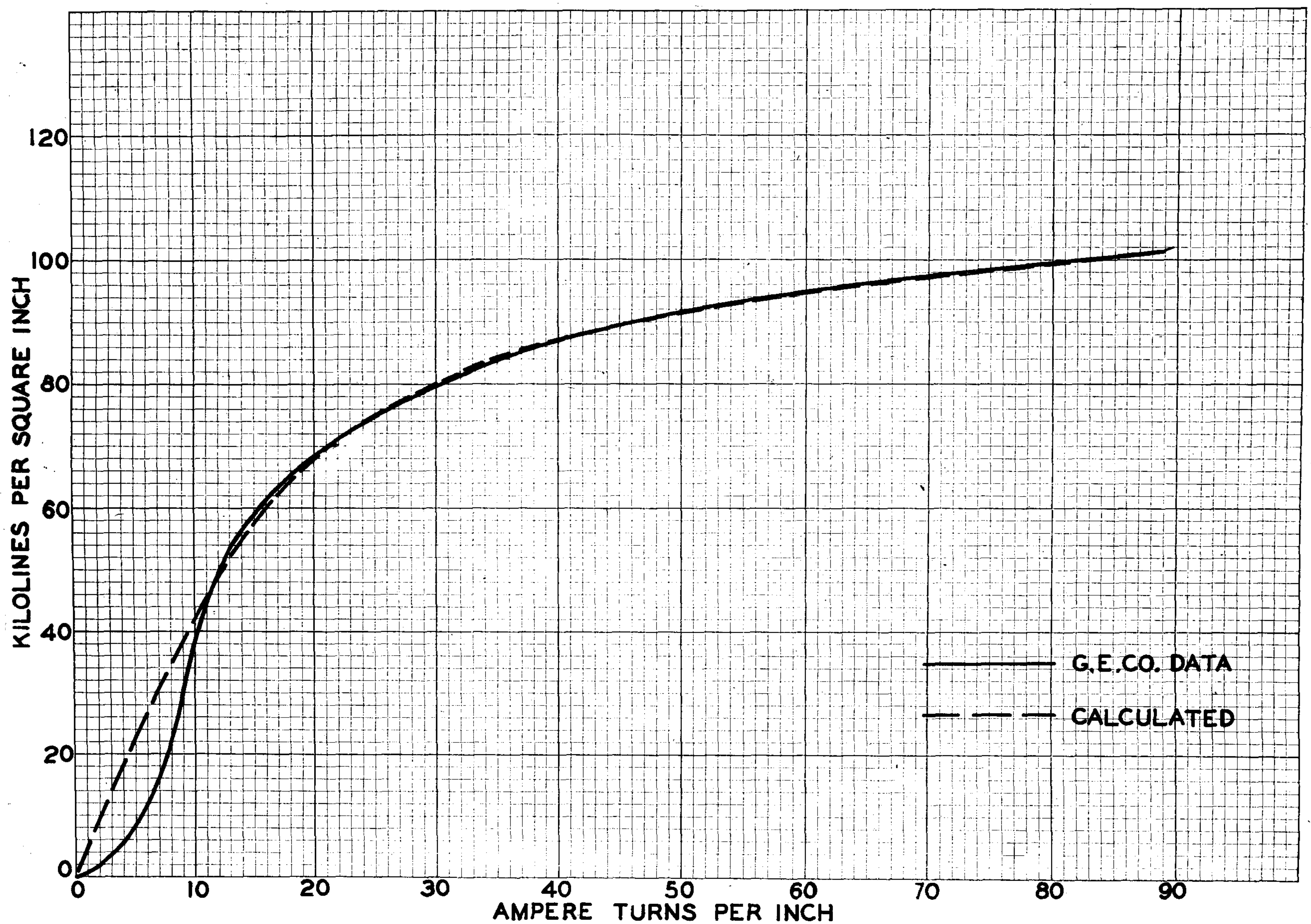

Fig. 4. Magnetization Curve for Common Sheet Steel.

III. APPLICATION TO THE THEORY OF FERRO-INDUCTANCE

A. Assumptions

In most modern magnetic steels the hysteresis loop has been very much reduced. Accordingly, its effect on magnetization of the steel has been neglected in order to simplify the mathematics. It was assumed that magnetization of the steel throughout an alternating current cycle took place along the normal magnetization curve, rather than around the hysteresis loop.

Leakage flux was also neglected, since it could not be accurately predicted. Later tests showed it to be very small, at least for the better steels with the core arrangements used.

B. Permeability

1. Normal or d-c permeability.

Normal permeability is the term used to describe the permeability obtained from the relation:

$$\mu = \frac{B}{H} \tag{20}$$

It is the slope of the straight line drawn from the origin of the magnetization curve to the point at which the permeability is desired. This is the useful permeability in direct current problems.

The normal permeability can be calculated from the empirical equation (9). Since:

$$B = B_n \, gd \, \frac{aNi'}{l} + \frac{cNi'}{l}$$

$$B = \mu H = \mu \frac{Ni'}{l}$$

$$\mu = \frac{B_n \, gd \, \frac{aNi'}{l}}{\frac{Ni'}{l}} + c = \frac{a \, B_n \, gd \, \frac{aNi'}{l}}{\frac{aNi'}{l}} + c \qquad (21)$$

Let $\frac{aNi'}{l} = \alpha$

then $\mu = (a B_n \, gd \, \alpha)/\alpha + c$ English units.

To convert this value of μ, which is in English units, to the more common relative permeability it must be multiplied by 0.3125. Then:

$$\mu = 0.3125 \left(\frac{a B_n \, gd \alpha}{\alpha} + c \right) \qquad (22)$$

A curve of values of $(gd\,\alpha)/\alpha$ plotted against α is of help in readily calculating the value of normal permeability for any value of magnetizing force. Such a curve is presented in Figure 5.

Equation (22) has been used to calculate the normal permeability of the Hipersil steel core whose magnetization curve is shown on Figure 2. The value of the iron constants a, B_n, and c are given in equation (17). A comparison of the

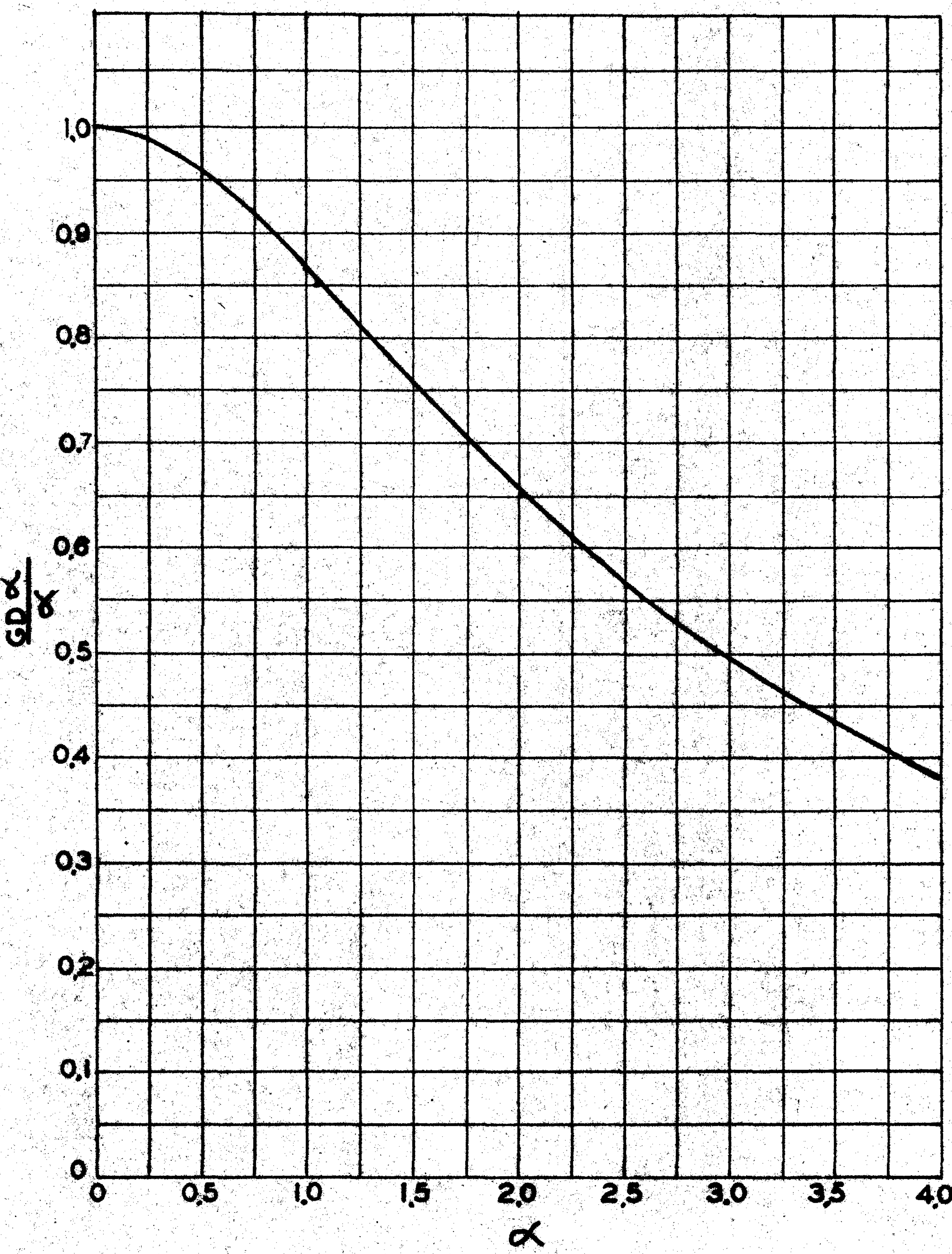

Fig. 5. The Function gd α/α .

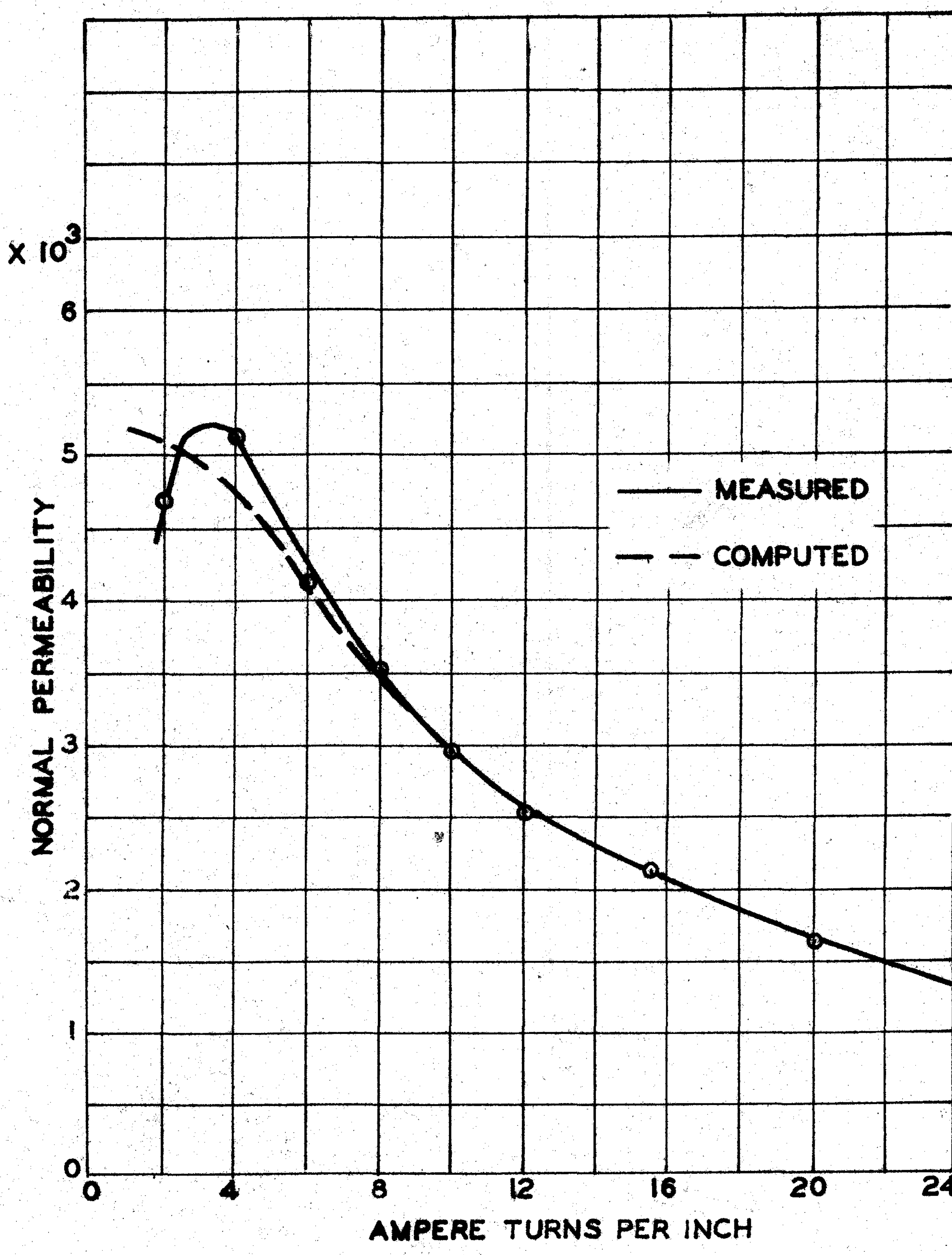

Fig. 6. Normal Permeability of Hipersil Steel.

TABLE 4

Value of gdα as a Function of α.

α	gdα	$\frac{gd\alpha}{\alpha}$
0.2	0.199	0.995
0.4	0.390	0.975
0.6	0.567	0.945
0.8	0.726	0.908
1.0	0.866	0.866
1.5	1.132	0.754
2.0	1.302	0.651
2.5	1.407	0.564
3.0	1.471	0.491
3.5	1.510	0.432
4.0	1.534	0.384
5.0	1.557	0.311
6.0	1.566	0.261
8.0	1.571	0.196

TABLE 5

Normal Permeability of Hipersil Steel

Amp.turns per inch	μ Measured English units	μ Measured Relative	μ Calculated Equation (23) Relative
2	15,000	4700	5060
4	16,400	5140	4750
6	13,250	4150	4090
8	11,250	3530	3470
10	9,550	2980	2990
12	8,200	2560	2590
15	6,800	2130	2140
20	5,250	1640	1640
30	3,600	1130	1070

calculated results with the measured values of μ taken from Figure 2 is made in Table 5 and Figure 6. Excellent agreement is shown indicating equation (22) is suitable for accurate computation of μ. Equally close agreement has been obtained for Nicaloi steel.

2. Differential or a-c permeability.

Differential permeability is defined as the slope of the magnetization curve, or the permeability to small changes of magnetizing force. That is:

$$\mu_d = \frac{dB}{dH} = \frac{dB}{d\frac{Ni}{l}}$$

and

$$B = B_n \, gd \, \frac{aNi}{l} + \frac{cNi}{l} \qquad (9)$$

Then μ_d, after multiplying by 0.3125 to convert to relative permeability, is:

$$\mu_d = 0.3125\left(a B_n \operatorname{sech} \frac{aNi}{l} + c\right) \qquad (23)$$

This value of permeability is of use in many a-c calculations.

To show that equation (23) is correct, Figure 7 for Hipersil steel and Figure 8 for Nicaloi have been prepared. The close agreement between the values of μ_d calculated from equation (23) and the μ_d measured from the slope of the actual magnetization curves is shown. The values of the iron constants a, B_n, and c are those of (17) and (18).

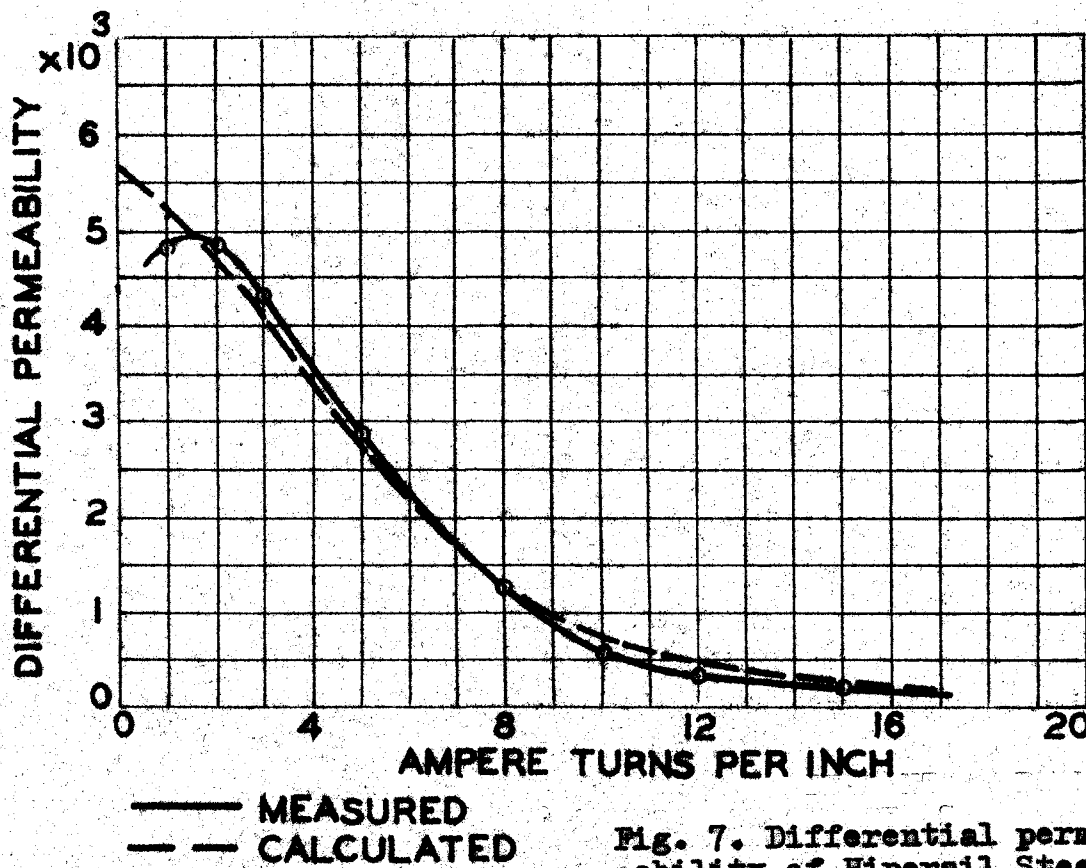

Fig. 7. Differential permeability of Hipersil Steel.

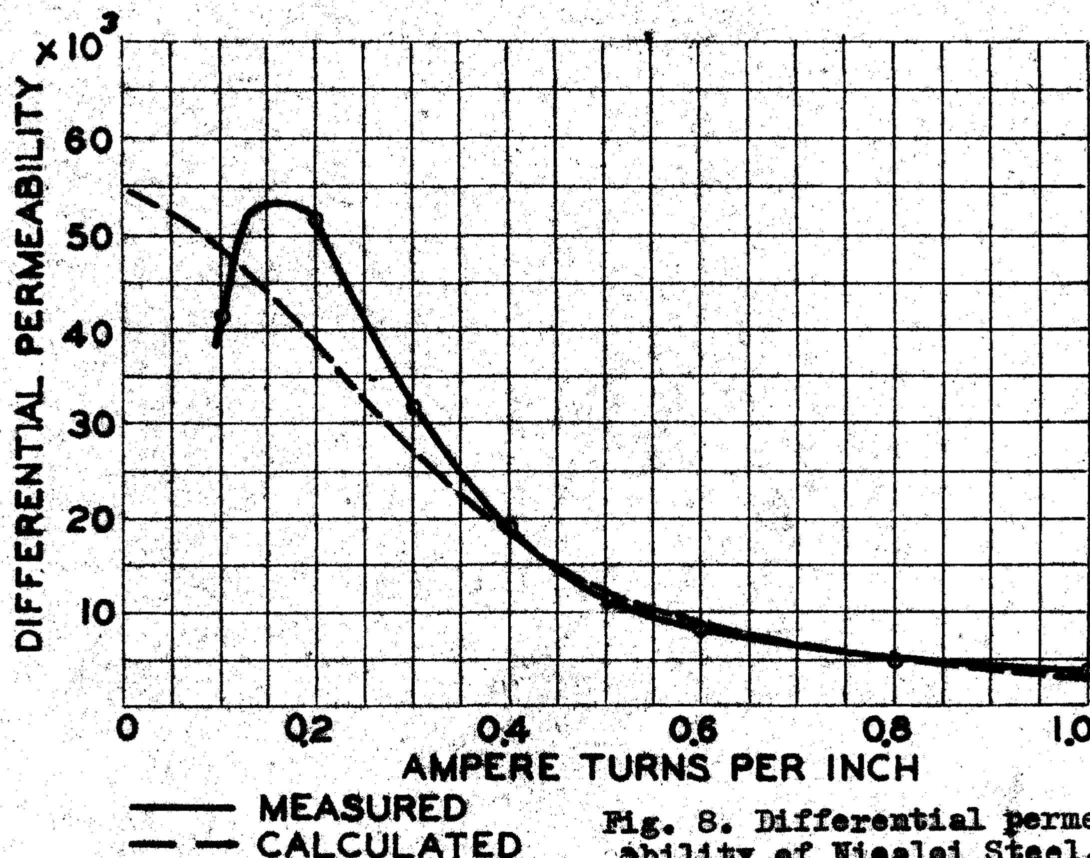

Fig. 8. Differential permeability of Nicaloi Steel.

TABLE 6

Differential Permeability of Hipersil Steel

Amp.turns per inch	μ_d Measured English units	μ_d Measured Relative	μ_d Calculated (23) Relative
0	14,100	4,400	5,680
1	15,300	4,780	5,190
2	15,600	4,870	4,860
3	13,800	4,310	4,130
5	9,200	2,880	2,660
8	4,000	1,250	1,300
10	1,780	556	775
12	1,140	356	470
15	700	219	240

TABLE 7

Differential Permeability of Nicaloi Steel

Amp.turns per inch	μ_d Measured English units	μ_d Measured Relative	μ_d Calculated (23) Relative
0.1	132,000	41,200	49,000
0.2	166,000	51,800	37,800
0.3	102,000	31,800	26,800
0.4	61,000	19,000	18,200
0.5	36,300	11,300	12,400
0.6	25,000	7,800	8,600
0.8	16,000	5,000	4,600
1.0	12,100	3,780	2,980
1.6	5,800	1,810	1,930

The slight departure of the curves at low values of Ni/l is due to the reverse curvature of the magnetization curves at low values, which equation (9) as the approximation does not match.

C. Ferro-inductance

1. Theory

The equation adopted for the magnetization curve is:

$$B = B_n \, gd \, \frac{aNi}{l} + \frac{cNi}{l}$$

Equation (7) states that:

$$L = N \frac{d\phi}{di} \times 10^{-8}$$

and

$$\phi = AB = AB_n \, gd \, \frac{aNi}{l} + \frac{cANi}{l} \qquad (24)$$

$$\frac{d\phi}{di} = \frac{aAB_nN}{l} \operatorname{sech} \frac{aNi}{l} + \frac{cAN}{l}$$

Then:

$$L = \frac{aAB_nN^2}{10^8 l} \operatorname{sech} \frac{aNi}{l} + \frac{cAN^2}{10^8 l} \qquad (25)$$

Equation (25) gives the value, in henrys, of the inductance of a ferro-inductor with any value of current flowing. The first term on the right is the contribution due to the presence of the iron, the second term is the constant value of the inductance if the iron is removed, leaving an air core.

Since the maximum value of sech x is unity and occurs for x equal to zero, then the maximum value of the inductance occurs at zero current and is:

$$L_{max} = \frac{aAB_nN^2}{10^8 l} + \frac{cAN^2}{10^8 l} \qquad (26)$$

Actually, due to the small reverse curvature of the magnetization curve near zero, the maximum measured inductance occurs not at but near zero. Ordinarily this discrepancy is so small as to be overlooked, but it is interesting to note that the value as given by (26) usually is very close to the maximum measured value of inductance.

By noting that sech ∞ equals zero, the value of inductance is seen to be never less than cAN^2/l, or that of the coil with an air core. High values of current can reduce the effectiveness of the iron to zero, but can never reduce the inductance value below that of the coil on an air core.

The equation (25) is a simple expression for the calculation of ferro-inductance. By its use an inductor can be designed in advance of construction, to have a given inductance at a given value of current, the only data required being the constants a, B_n and c of the particular type of iron to be used.

The accuracy of (25) is demonstrated in the following sections.

2. Methods of measurement of ferro-inductance

The statement of Hanna[7], that the inductance of ferro-inductors should be measured with a small a-c voltage, or the Bell Laboratories Record[23] statement, that ferro-inductors can be measured only under actual operating conditions of current and voltage, both indicate the lack of precise knowledge and the difficulties to be encountered in the measurement of ferro-inductance.

Ordinary a-c bridge methods, whether used with a small a-c voltage or not, are not suitable. The voltage applied to the inductor varies as the bridge is balanced, changing the value of inductance, which changes the balance value and results in a sliding balance point. This is especially true for high permeability steels. If balance is reached, knowledge of the actual current flowing through the reactor is not obtainable, and the value of inductance means nothing.

A bridge especially designed for this[23], and including means of measuring a-c and d-c currents still overlooks a fundamental point. It may give information on the effective inductance under the particular operating conditions but it gives no clue to a means for determining the inductance under quite different operating conditions. Such a bridge actually measures the slope of the major axis of the hysteresis loop being traced in the iron. This slope is not a simple function of the current flowing, so that data cannot be extrapolated to a different set of current conditions.

Measurements of inductance by measurement of impedance, using very small values of a-c voltage, are not satisfactory, always giving values lower than predicted by (25). This is again due to the fact that the a-c method is measuring the slope of the major axis of the hysteresis loop, and this slope is always less than that of the magnetization curve at the point, yielding a lower inductance value.

Equation (25), however, provides a means for calculating the inductance under any desired set of conditions, and therefore is a more fundamental and basic relationship.

It was necessary to develop a new method by which ferro-inductance could be measured at any value of current or ampere turns. This new method was based on the relationship:

$$L = N \frac{d\phi}{di} \times 10^{-8}$$

From this, it can be seen that the inductance can be measured at any value of steady ampere turns, if a differential change in current be made, the resulting differential change in flux measured, and the ratio taken and multiplied by N.

For accurate measurements of the differential current change it is most convenient to use a three coil arrangement as shown in the circuit diagram of Figure 9. The steady d-c ampere turns are applied in coil N_1, the differential current change is made in coil N_2 whose inductance is to be measured, and the third coil N_3 is for ballistic measurement of the flux change with a galvanometer. The ampere turns of the first and

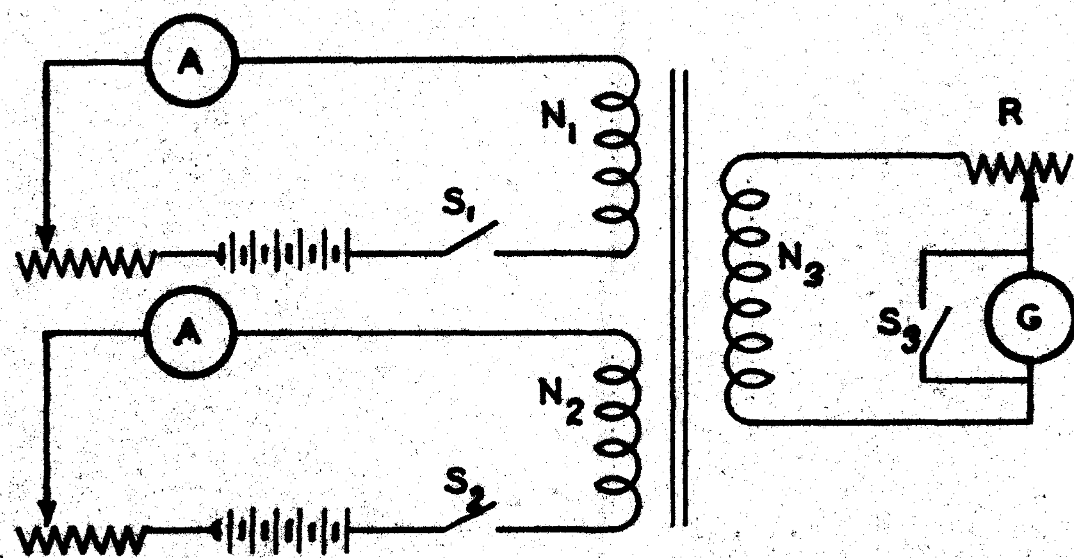

N_2 AMPERE TURNS MUST AID N_1 AMPERE TURNS

Fig. 9. Circuit for Measurement of Ferro-inductance.

second coils must be connected to aid.

The procedure for measuring the value of inductance at one value of steady ampere turns is as follows:

With switch S_3 closed, open switch S_1, and close switch S_2 and adjust the value of current to give the desired differential ampere turns in coil N_2. Open switch S_2.

Demagnetize the core thoroughly with a heavy application of a-c ampere turns which are slowly reduced to zero. Close switch S_1 and increase the current to give the desired value of d-c ampere turns at which the inductance is to be obtained. This value must always be approached from below, and if passed accidentally the core must be demagnetized and the procedure repeated.

Open the galvanometer shorting switch S_3, then close switch S_2 and read the resulting ballistic throw of the galvanometer. By use of the galvanometer calibration constant K, the flux change can be obtained and substituting in

$$L = N \frac{d\phi}{di} \times 10^{-8},$$

where N is N_2, the turns in the current change coil, the inductance is easily computed.

The method is based on the fact that after demagnetization, an iron core is magnetized along the normal magnetization curve, and the differential change is made in an additive manner, taking the iron further along the normal curve. In this way the effect of a hysteresis loop is eliminated and the inductance is measured in a manner agreeing with the theory and the assumptions.

The galvanometer can be calibrated by use of a mutual inductance, but since capacitors were more readily available they were used. The deflection α of a ballistic galvanometer is proportional to the charge Q that passes through the galvanometer

$$Q = K\alpha$$

If a condenser of known capacity C is charged to a known voltage E then:

$$Q = CE$$

and the constant K becomes:

$$K = \frac{CE}{\alpha} \quad \text{coulombs/cm.} \qquad (27)$$

For the galvanometer used this constant was determined as 0.215×10^{-6} coulombs per centimeter.

The charge Q passing through a ballistic galvanometer when the flux linkages in the circuit change from $N\phi_1$ to $N\phi_2$ is given by:

$$Q = \frac{N\phi_1 - N\phi_2}{R} = \frac{N\Delta\phi}{R} \qquad (28)$$

where R is the resistance of the ballistic circuit. Equation (28) gives a result in electromagnetic units, but a change to practical units gives:

$$Q = \frac{N\Delta\phi}{10^8 R} \quad \text{coulombs} \qquad (29)$$

and since

$$Q = K\alpha$$

then

$$N \Delta\phi = RK\alpha \times 10^{8} \tag{30}$$

is an expression relating the galvanometer deflection to the change in flux linkages producing it. This equation (30) serves to calculate the $\Delta\phi$ change in flux produced by the differential change of current.

Since the differential current and flux changes must be measured in finite quantities the question arises of how large can a differential change be. It would seem reasonable that the smaller the size of the change, the nearer it comes to being infinitesimal, the more correct would be the results. Or, that as the size of the change was reduced, the inductance measured would approach a constant value. In practice this turns out not to be the case; the differential change can be made too small. The reason for this has not been determined but may be due to steel characteristics or the apparatus used.

The curve of Figure 10 shows the inductance values measured for one particular coil when the size of the differential change of ampere turns was varied. It can be seen that if the differential change is too small, the inductance measured is low, but as the differential change is increased the value of inductance rises and reaches a constant value, then begins to decline as the change becomes quite large. The

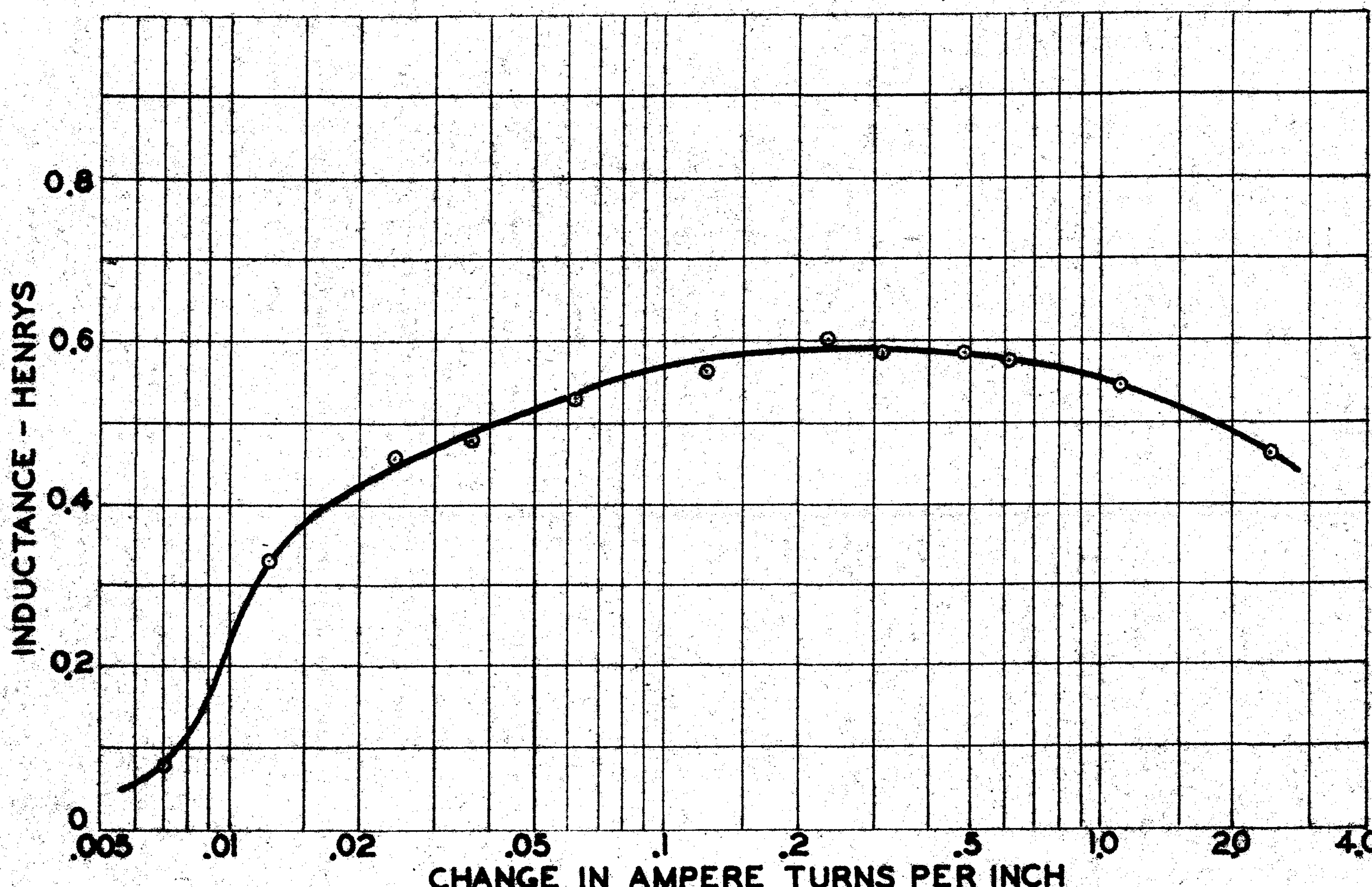

Fig. 10. Effect of the magnitude of the differential change on measured inductance.

value of inductance in the plateau region checks that predicted from calculation.

All subsequent measurements were made with changes of ampere turns which placed the point of operation well in the plateau region of Figure 10.

TABLE 8

Variation of Measured Inductance as a Function of the Size of $\Delta Ni/l$, Hipersil Core

Ampere turns/inch Change	L Henrys
0.007	0.082
0.012	0.334
0.024	0.459
0.037	0.484
0.061	0.533
0.12	0.558
0.22	0.601
0.31	0.585
0.49	0.583
0.61	0.572
1.16	0.547
2.40	0.467

3. <u>Experimental results</u>

If (25)

$$L = \frac{aAB_u N^2}{10^8 l} \operatorname{sech} \frac{aN_i'}{l} + \frac{cAN^2}{10^8 l} \qquad (25)$$

does accurately predict the value of inductance of a coil at any value of ampere turns per inch, then the results of the measurements made by the method just described should check values computed from (25).

Tests were run using the Hipersil core with constants:

a - 0.273

B_n - 65,000

c - 180

l - 13.15 inches

A - 1.87 square inches

The tests were with a coil of 156 turns, using a $\Delta Ni/l$ of both 0.118 and 0.236 ampere turns per inch with identical results; and a coil of 312 turns using a $\Delta Ni/l$ of 0.236 ampere turns per inch. The results of these tests are shown by the solid line curves in Figures 11 and 12, compared with the theoretical dashed line curves computed from (25) using the constants above for Hipersil steel. Tables 9 and 11 show the sets of data taken for the solid curves of Figures 11 and 12, using the method developed for measuring the value of ferro-inductance.

Close agreement between measured and computed values is obtained over most of the range, resulting in a satisfactory check of the theory. These curves substantiate also the measuring method developed to obtain this data.

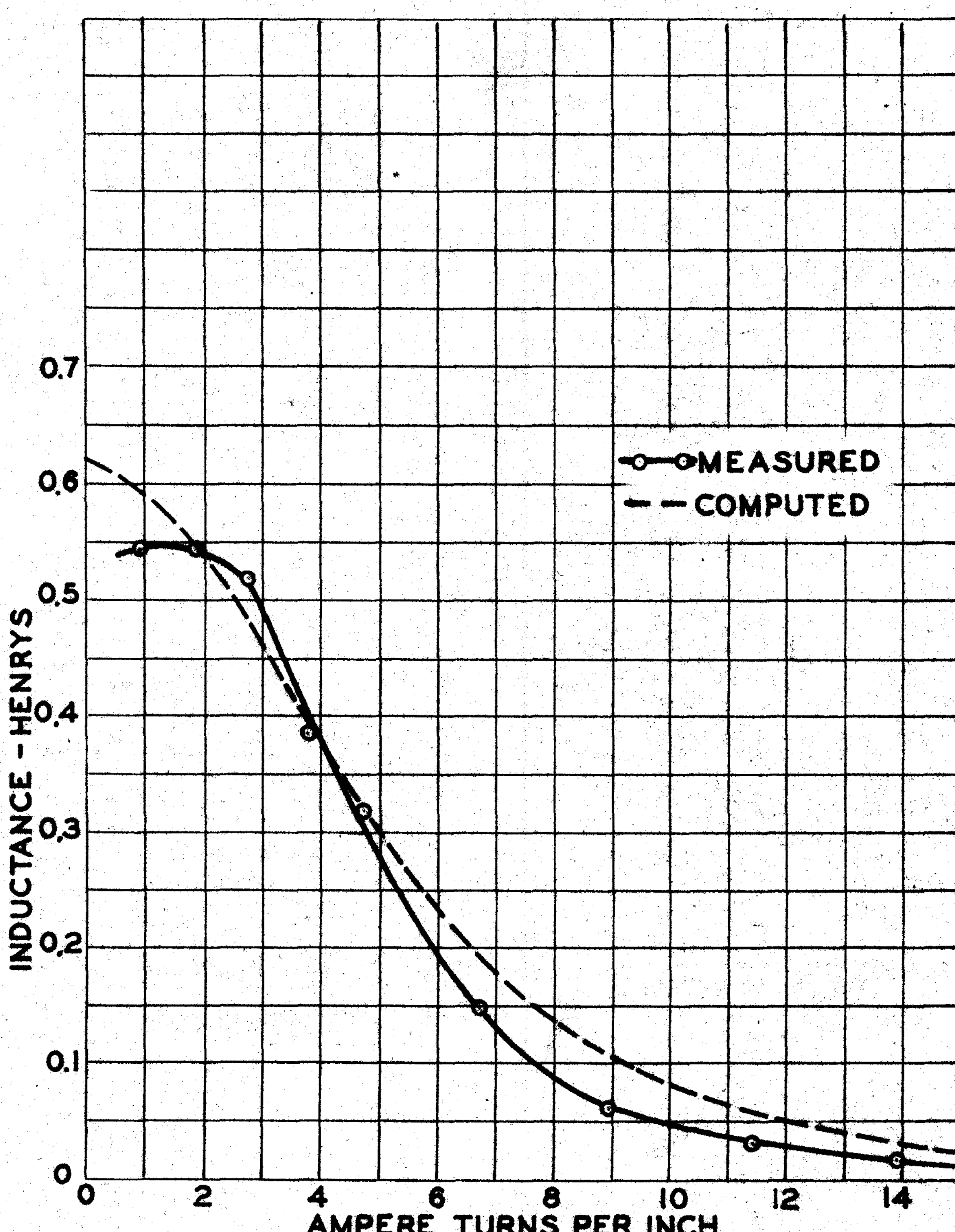

Fig. 11. Inductance of Reactor #1, 156 turns on Hipersil Core.

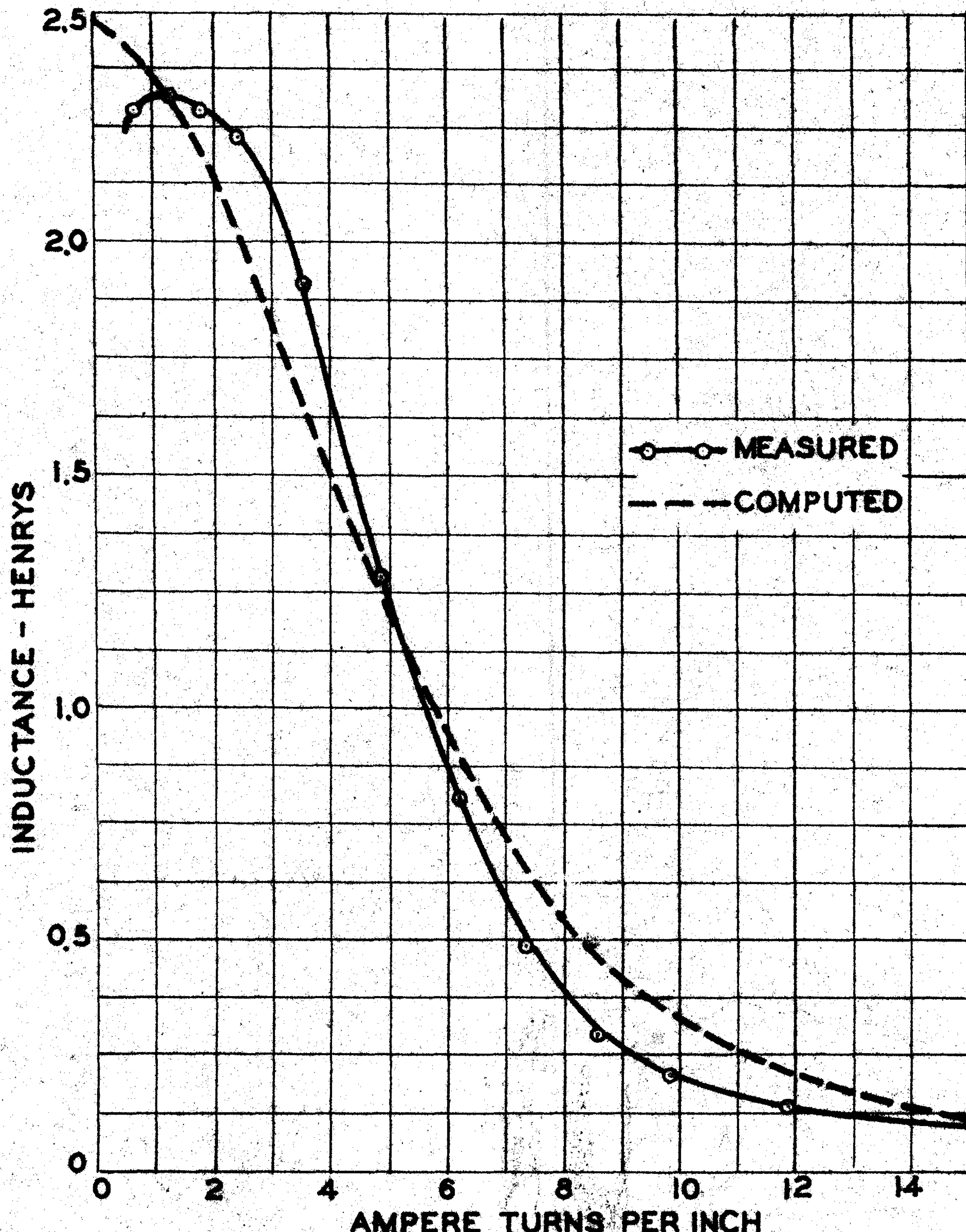

Fig. 12. Inductance of 312 turn Coil on Core of Reactor #1.

TABLE 9

Measurement of Ferro-inductance

Reactor #1, 156 turns on Hipersil Core

Amp.turns per inch $N_1 = 312$	I_{d-c} $N_2 = 156$	Galv.throw Cm. * $N_3 = 968$	R Ohms	$\Delta N_3\phi$ X10[6]	$\Delta\phi$	$\Delta N_2\phi$ X10[6]	L Henrys
0.95	0.010	15.5	10,170	3.38	3500	0.54	0.54
1.90	"	15.5	"	3.38	3500	0.54	0.54
2.87	"	14.8	"	3.23	3340	0.52	0.52
3.82	"	10.9	"	2.39	2470	0.39	0.39
4.77	"	9.1	"	1.98	2050	0.32	0.32
6.73	"	4.2	"	0.92	948	0.15	0.15
8.95	"	3.4	5,170	0.38	395	0.06	0.06
11.4	"	7.8	1,170	0.20	202	0.03	0.03
13.9	"	5.0	"	0.13	130	0.02	0.02
16.9	"	3.7	"	0.09	97	0.015	0.015

* Galvanometer K = 0.215×10^{-6}

TABLE 10

Calculated Ferro-inductance

Reactor #1, 156 turns on Hipersil Core

Amp.turns per inch	$\frac{aNi}{l}$	sech $\frac{aNi}{l}$	180 $\frac{N^2A}{l}$	$\frac{aAB_nN^2}{10^8\, l}\operatorname{sech}\frac{aNi}{l}$	L Henrys
0	0.000	1.000	0.0062	0.615	0.621
2	0.546	0.865	0.0062	0.532	0.538
3	0.819	0.738	"	0.454	0.460
4	1.092	0.603	"	0.371	0.377
5	1.365	0.479	"	0.294	0.300
7	1.911	0.290	"	0.178	0.184
9	2.457	0.170	"	0.105	0.111
12	3.280	0.075	"	0.046	0.052
15	4.090	0.033	"	0.020	0.026

TABLE 11

Measurement of Ferro-inductance

Reactor #1, 312 turns on Hipersil Core

Amp.turns per inch $N_1 = 156$	I_{dc} $N_2 = 312$	Galv.throw Cm. $N_3 = 968$	R Ohms	$\Delta N_3 \phi$ X10^6	$\Delta \phi$	$\Delta N_2 \phi$ X10^6	L Henrys
0.6	0.010	16.3	20,170	7.06	7320	2.27	2.27
1.2	"	16.5	"	7.15	7410	2.30	2.30
1.8	"	16.3	"	7.06	7320	2.27	2.27
2.4	"	16.0	"	6.92	7180	2.23	2.23
3.6	"	13.6	"	5.89	6100	1.90	1.90
4.9	"	9.1	"	3.94	4080	1.27	1.27
6.1	"	11.4	10,170	2.49	2580	0.80	0.80
7.3	"	6.9	"	1.51	1560	0.49	0.49
8.6	"	8.5	5,170	0.94	970	0.30	0.30
9.9	"	5.8	"	0.65	668	0.21	0.21
11.9	"	8.8	2,170	0.41	429	0.13	0.13

TABLE 12

Calculated Ferro-inductance

Reactor #1, 312 turns on Hipersil Core

Amp.turns per inch	$\frac{aNi}{l}$	sech $\frac{aNi}{l}$	180 $\frac{N^2A}{l}$	$\frac{aAB_nN^2}{10^8\,l}$ sech $\frac{aNi}{l}$	L Henrys
0	0.000	1.000	0.0249	2.46	2.48
2	0.546	0.866	"	2.13	2.15
4	1.092	0.603	"	1.48	1.50
6	1.638	0.374	"	0.92	0.94
8	2.184	0.222	"	0.54	0.56
10	2.730	0.130	"	0.32	0.34
12	3.276	0.075	"	0.18	0.20
15	4.095	0.036	"	0.09	0.11

D. Energy Storage

The energy stored magnetically in an inductance is frequently of importance. An expression for this can readily be obtained. Neglecting resistance voltage drops, the energy stored in a ferro-inductor is given by:

$$\text{Energy} = \mathcal{E} = \int_0^t e\, i\, dt$$

$$= \int_0^t \frac{N}{10^8} \frac{d\phi}{dt}\, i\, dt = \frac{N}{10^8} \int_0^\phi i\, d\phi$$

and if the $eAN^2/10^8 l$ term is neglected in the ferro-inductance relation (25), then:

$$\phi = AB_n \, gd \, \frac{aNi}{l}$$

$$i = \frac{l}{aN}\, gd^{-1} \frac{\phi}{AB_n}$$

then

$$\mathcal{E} = \frac{N}{10^8} \int_0^\phi \frac{l}{aN}\, gd^{-1} \frac{\phi}{AB_n}\, d\phi$$

The anti-gudermannian may be expanded as a series:

$$gd^{-1} \frac{\phi}{AB_n} = \frac{\phi}{AB_n} + \frac{1}{6}\left(\frac{\phi}{AB_n}\right)^3 + \frac{1}{24}\left(\frac{\phi}{AB_n}\right)^5 + \frac{61}{5040}\left(\frac{\phi}{AB_n}\right)^7 + \text{-----} \qquad (32)$$

Upon inserting this series and integrating, the energy becomes:

$$\mathcal{E} = \frac{l}{10^8 a}\left[\frac{\phi^2}{2AB_n} + \frac{1}{24}\frac{\phi^4}{(AB_n)^3} + \frac{1}{144}\frac{\phi^6}{(AB_n)^5} + \frac{61}{40320}\frac{\phi^8}{(AB_n)^7} + \cdots\right]$$

The energy expressed as a function of flux is in an inconvenient form, but flux may be expressed as a function of current and the expression becomes:

$$\mathcal{E} = \frac{AB_m l}{10^8 a}\left[\frac{gd^2 \frac{aNi'}{l}}{2} + \frac{gd^4 \frac{aNi'}{l}}{24} + \frac{gd^6 \frac{aNi'}{l}}{144} + \frac{61}{40320} gd^8 \frac{aNi'}{l} + \cdots\right] \quad (33)$$

This is the energy stored in the magnetic field during a change in current from zero to i.

E. Value of Inductance for Applied Sinusoidal EMF

Consider the circuit:

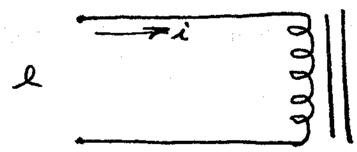

with

$$e = E_m \cos \omega t$$

and neglecting the resistance of the reactor and circuit, an equation for the flux present in the iron can be written:

$$\phi = \frac{10^8}{N}\int e\,dt = \frac{10^8}{N}\int E_m \cos \omega t\,dt$$

$$\phi = \frac{E_m}{N\omega} \sin \omega t \times 10^8 \quad (34)$$

By the expression for the magnetization curve:

$$\phi = AB_n\, gd\, \frac{aNi'}{l} + \frac{cANi^3}{l}$$

and ordinarily the last term on the right can be neglected as very small. This term will be neglected in much of the material that follows.

Then:

$$\phi = A B_n \, gd \, \frac{aN_i'}{l}$$

$$gd \, \frac{aN_i'}{l} = \frac{\phi}{AB_n}$$

From the properties of the gudermannian a right triangle can be drawn (see Part II, section B).

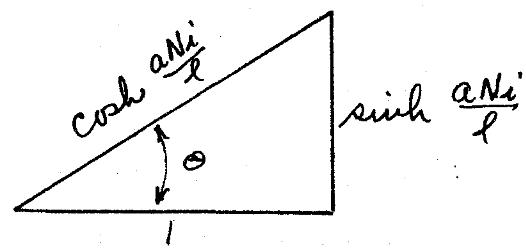

where

$$\theta = gd \, \frac{aN_i'}{l} = \frac{\phi}{AB_n}$$

and from which it can be seen that:

$$\frac{1}{\cosh \frac{aN_i'}{l}} = \operatorname{sech} \frac{aN_i'}{l} = \cos \frac{\phi}{AB_n} \qquad (35)$$

Substituting (34) into (35):

$$\operatorname{sech} \frac{aN_i'}{l} = \cos \frac{E_m 10^8 \sin \omega t}{\omega A B_n N} \qquad (36)$$

Then equation (25) for ferro-inductance, again neglecting the term containing e, becomes:

$$L = \frac{a A B_n N^2}{10^8 l} \operatorname{sech} \frac{aN_i'}{l} = \frac{a A B_n N^2}{10^8 l} \cos \frac{E_m 10^8 \sin \omega t}{\omega A B_n N} \qquad (37)$$

Now it is known that:

$$\cos (x \sin v) = J_0(x) + 2\, J_2(x) \cos 2v + 2\, J_4(x) \cos 4v + \cdots$$

where $J_0(x)$, $J_2(x)$, $J_4(x)$..... are Bessel function coefficients which can be readily evaluated from tables of the function. Consequently the expression for inductance becomes:

$$L = \frac{aAB_nN^2}{10^8 l}\left[J_0\left(\frac{E_m 10^8}{\omega AB_nN}\right) + 2J_2\left(\frac{E_m 10^8}{\omega AB_nN}\right)\cos 2\omega t + 2J_4\left(\frac{E_m 10^8}{\omega AB_nN}\right)\cos 4\omega t + \text{-----}\right] \quad (38)$$

This shows that, for a sinusoidal applied voltage, the inductance of a ferro-inductor consists of a constant term plus sinusoidally varying terms in even harmonics of the applied frequency. This provides an explanation of the source of the harmonic components appearing in the current that flows through the reactor.

F. Current Flowing in a Ferro-inductor, Sine EMF Applied

Again assume an emf of:

$$e = E_m \cos \omega t$$

applied to a ferro-reactor and neglect the resistance of the circuit, also the GNi/l term of the flux equation. Then from the preceding section the flux is given by (34):

$$\phi = \frac{10^8 E_m}{\omega N} \sin \omega t$$

also

$$\phi = AB_m \, gd \, \frac{aNi}{l} = \frac{10^8 E_m}{\omega N} \sin \omega t$$

$$gd \, \frac{aNi}{l} = \frac{10^8 E_m}{\omega A B_m N} \sin \omega t$$

$$i = \frac{l}{aN} \, gd^{-1} \left(\frac{10^8 E_m}{\omega A B_m N} \sin \omega t \right) \tag{39}$$

Equation (39) is an expression for the current that will flow in the reactor under the assumptions. It will always be larger than the actual current due to the neglection of the effective resistance of the reactor. Because of the nature of gd^{-1} it is obviously non-sinusoidal.

Frequently it is very desirable to be able to calculate the values of the harmonic components present in the current and these can be obtained by further analysis. The series expansion for the anti-gudermannian is:

$$gd^{-1} u = u + \frac{u^3}{6} + \frac{u^5}{24} + \frac{61 u^7}{5040} + \text{-------} \tag{40}$$

Then writing for simplicity:

$$G = \frac{10^8 E_m}{\omega A B_m N} \tag{41}$$

equation (39) becomes:

$$i = \frac{l}{aN} \left[G \sin \omega t + \frac{G^3}{6} \sin^3 \omega t + \frac{G^5}{24} \sin^5 \omega t + \frac{61 G^7 \sin^7 \omega t}{5040} + \cdots \right] \tag{42}$$

By substituting for the trigonometric relations their identities in terms of multiple angles:

$$i = \frac{l}{aN}\Big[G \sin \omega t + \frac{G^3}{16}\left(\frac{3}{4}\sin \omega t - \frac{1}{4}\sin 3\omega t\right)$$
$$+ \frac{G^5}{24}\left(\frac{1}{16}\sin 5\omega t - \frac{5}{16}\sin 3\omega t + \frac{5}{8}\sin \omega t\right)$$
$$+ \frac{61 G^7}{5040}\left(-\frac{\sin 7\omega t}{64} + \frac{7}{64}\sin 5\omega t + \frac{21}{64}\sin 3\omega t + \frac{35}{64}\sin \omega t\right)$$
$$+ \text{-----------------------}\Big]$$

and after collecting terms:

$$i = \frac{l}{aN}\Big[\left(G + \frac{G^3}{8} + \frac{5G^5}{192} + \frac{2135\, G^7}{322000} + \text{-----}\right)\sin \omega t$$
$$-\left(\frac{G^3}{24} + \frac{5G^5}{384} + \frac{1280\, G^7}{322000} + \text{-----}\right)\sin 3\omega t$$
$$+\left(\frac{G^5}{384} + \frac{427 G^7}{322000} + \text{---------}\right)\sin 5\omega t$$
$$-\left(\frac{61 G^7}{322000} + \text{---------}\right)\sin 7\omega t + \text{------}\Big] \qquad (43)$$

Equation (43) gives the values to be expected for each harmonic component in the current. It shows that the frequencies are odd harmonics, and alternate in algebraic sign, as is well known for this case.

In Table 13 is presented an analysis of input current waveforms for sine applied voltage. The analysis was made with a General Radio Wave Analyzer. For comparison there is also presented the calculated analysis of the current waves, using equation (43). Reasonable accuracy is obtained, and could no doubt be improved if more terms of the anti-gudermannian series were taken, since the terms in some of the harmonic coefficients converge rather slowly.

TABLE 13

Harmonic Analysis - Input Current

Reactor #1 - 156 turns, Hipersil Core

	Voltage applied 60 rms		Voltage applied 83 rms.	
	Measured	Calculated	Measured	Calculated
RMS total I	0.27	0.31	0.40	0.53
Fundamental %	100.0	100.0	100.0	100.0
Third Harmonic %	7.8	7.5	20.4	17.5
Fifth Harmonic %	1.8	0.7	6.7	2.7
Seventh Harmonic %	0.4	0.4	3.1	2.1

One other important source of error is represented. Equation (43) was developed under an assumption of negligible resistance. Actually it is impossible to separate a ferro-reactance from its associated effective resistance for purposes of measurement. The effective resistance of reactor #1 is not negligible and consequently the actual currents flowing are less than predicted by theory. The effective resistances are approximately 32 ohms for the 60 volt case and

20 ohms for 83 applied volts.

Equation (43) does have considerable value, however, since there is no other method available for determining the current components or the total current.

IV. IMPEDANCE OF A CIRCUIT CONTAINING A FERRO-INDUCTOR

A. Instantaneous Circuit Equations

Assume a circuit containing a ferro-inductor in series with a resistance R and a capacitor C.

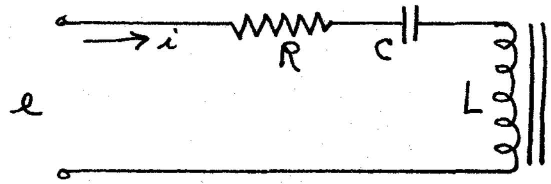

A current i is assumed to flow and the differential equation of the circuit may be written as:

$$L\frac{di}{dt} + Ri + \frac{1}{C}\int i\,dt = e \qquad (44)$$

Since the term cAN^2/l may usually be neglected in the inductance equation, (25) may be written:

$$L = \frac{aAB_nN^2}{10^8 l}\,\mathrm{sech}\,\frac{aNi}{l}$$

For simplicity let:

$$D = \frac{aAB_nN^2}{10^8 l}$$

and then (44) becomes:

$$D\,\mathrm{sech}\,\frac{aNi}{l}\frac{di}{dt} + Ri + \frac{1}{C}\int i\,dt = e$$

This equation has so far been insoluble for the case where $e = E_m \sin\omega t$. If, however, a sinusoidal current is assumed

$$i = I_m \sin \omega t$$

$$\frac{di}{dt} = I_m \omega \cos \omega t$$

and substituting these values, (44) becomes:

$$\omega D I_m \operatorname{sech}\left(\frac{aNI_m \sin\omega t}{l}\right) \cos\omega t + RI_m \sin\omega t - \frac{I_m}{\omega C} \cos\omega t = e$$

$$RI_m \sin\omega t + I_m\left(\omega D \operatorname{sech} \frac{aNI_m \sin\omega t}{l} - \frac{1}{\omega C}\right) \cos\omega t = e \qquad (45)$$

For equation (45) to be fulfilled, e must be non-sinusoidal. This equation is of little practical interest since ordinarily it is the voltage which is available as a sinusoid, not the current. By use of a distorted voltage, applied to such a circuit, a sine current could be obtained, but a different distorted voltage would be required for every case. This is impractical for general use.

B. Adaptation to RMS Values

Equation (45) is so similar in form to the conventional circuit equation:

$$RI + jI\left(\omega L - \frac{1}{\omega C}\right) = E \qquad (46)$$

involving rms values of current and voltage, that it should be possible in some manner to bridge the gap between the instantaneous quantities of (45) and the rms quantities of (46).

The value of L is seen to be the major difference in the two equations.

Inductance as determined by the ferro-inductance relation (25) is an instantaneous quantity, dependent on the instantaneous value of a varying current. Over a cycle of current variation the ferro-inductance changes through a considerable range of values. Its effect in the circuit, then, will be some sort of a weighted average of the values taken during the current cycle, or, through the ferro-inductance relation, a weighted function of the current or ampere turns.

The magnitude of the weighting factor will depend on the manner in which the inductance varies with the current and this is fixed by the magnetization curve. The factor in the inductance relation which reflects the shape of the magnetization curve is sech (aNi/l). Consequently if a weighting factor is present, it will appear in the angle of the hyperbolic secant as some factor "k". The effective value of inductance L_e then may be written as:

$$L_e = D \operatorname{sech} \frac{kaNI}{l} \tag{47}$$

where I is the rms value of current.

Based on this argument and the similarity between (45) and (46) it seems reasonable to assume:

$$I = \frac{E}{\sqrt{R^2 + \left(\omega D \operatorname{sech} \frac{kaNI}{l} - \frac{1}{\omega C}\right)^2}} \tag{48}$$

where E and I are effective values and k is the weighting factor for a particular steel.

The impedance of a ferro-inductive circuit then becomes:

$$Z = \sqrt{R^2 + \left(\omega D \operatorname{sech} \frac{kaNI}{l} - \frac{1}{\omega C}\right)^2} \tag{49}$$

for a particular value of effective current I. The resistance term R includes the effective resistance of the reactor as well as any external resistance in the circuit.

Since (48) is an assumption, experimental verification must be obtained.

C. Determination of Effective Resistance

Before computing the effective reactance of a ferro-inductor it is necessary to be able to calculate the effective resistance. Preferably, this should be done directly from the design data of coil and steel chosen.

It is customary to calculate the effective resistance R_e by definition:

$$R_e = \frac{W}{I^2} \tag{50}$$

where W is the wattage dissipated in the reactor and I the effective value of the fundamental component of current. However, the fundamental component is not easily obtained, the effective value of the distorted current waveform usually being the only information directly available.

When a ferro-inductor is in series with another impedance across a sinusoidal voltage, neither the current through nor the voltage across the ferro-inductor is sinusoidal, in general. Therefore the flux is not sinusoidal but is made up of the fundamental plus harmonic frequencies. The total iron losses vary as some power of the frequency, the exponent being between one and two. They also are considered a function of the peak flux density. The peak flux density can be measured by means of a peak reading vacuum tube voltmeter, if the magnetization curve is available, but this is not a convenient method. For convenience of measurement, the rms current, voltage and the power are most readily obtained. Consequently the relation between rms current or ampere turns and watts loss for such distorted flux waveforms would be interesting since it would reflect not only the variation of the iron losses with waveform, but also the variation of iron losses with peak flux or peak current.

A circuit using a resistance R in series with reactor #1, 156 turns, and voltmeter, wattmeter and ammeter was set up. Sinusoidal voltage of variable magnitude was applied from a source of excellent regulation. The resistance R was used in order to change the voltage waveform, and thus the harmonic content of the flux. The current waveform could be made to vary over a considerable range from almost sinusoidal with high series resistance and voltage, to distorted, with as high as 30% third harmonic, with zero resistance in series.

To determine whether rms current could be used as a parameter instead of the harder to measure peak flux density, data were taken for curves of iron losses plotted against both. Figure 13 shows the results of iron losses per pound of iron plotted against peak flux density for values of series resistance R varying from zero to five hundred ohms. This gives the variation in waveform mentioned above. The weight of the core of reactor #1 was 6.9 pounds. Figure 14 is a similar curve of iron losses per pound plotted against rms ampere turns per inch.

Figure 13 shows some variations as the waveform varies, indicating moderate changes of losses with percentage of flux harmonics. But figure 14 plotted against rms ampere turns per inch shows even less variation for the same wave form changes. Evidently the change in the losses with frequency is somewhat compensated by the accompanying change in peak factor of the current.

Since the rms current is so readily measured it seems desirable to use curves of watts loss per pound vs.rms ampere turns per inch as the basis for computing the effective resistance of ferro-reactors in the design process.

To compute the effective resistance of a reactor during the design of a circuit, equation (50) may be used with I as effective value:

$$R_e = \frac{W}{I^2} \tag{50}$$

If W, from previous measurements on the iron, can then be expressed in terms of rms ampere turns per inch, the effective resistance of a reactor for any value of current may be obtained.

Figure 14 can be approximated to a fair degree of accuracy by a power series of the form:

$$W/lb = K_1 \frac{NI}{l} + K_2 \left(\frac{NI}{l}\right)^2 + \text{-----} \qquad (51)$$

This then gives as an expression for R_e the equation:

$$R_e/lb = \frac{K_1 \frac{NI}{l} + K_2 \left(\frac{NI}{l}\right)^2}{I^2}$$

$$R_e/lb = \frac{K_1 N}{lI} + \frac{K_2 N^2}{l^2} \qquad (52)$$

One test of an iron is sufficient to obtain the constants K_1 and K_2.

For the Hipersil core a satisfactory average curve gave values for K_1 and K_2 which led to the equation:

$$W/lb = 0.213 \frac{NI}{l} - 0.00784 \left(\frac{NI}{l}\right)^2 + \text{--} \qquad (53)$$

A curve of this equation is shown dashed in Figure 14, drawn from data in Table 16. The effective resistance of a reactor

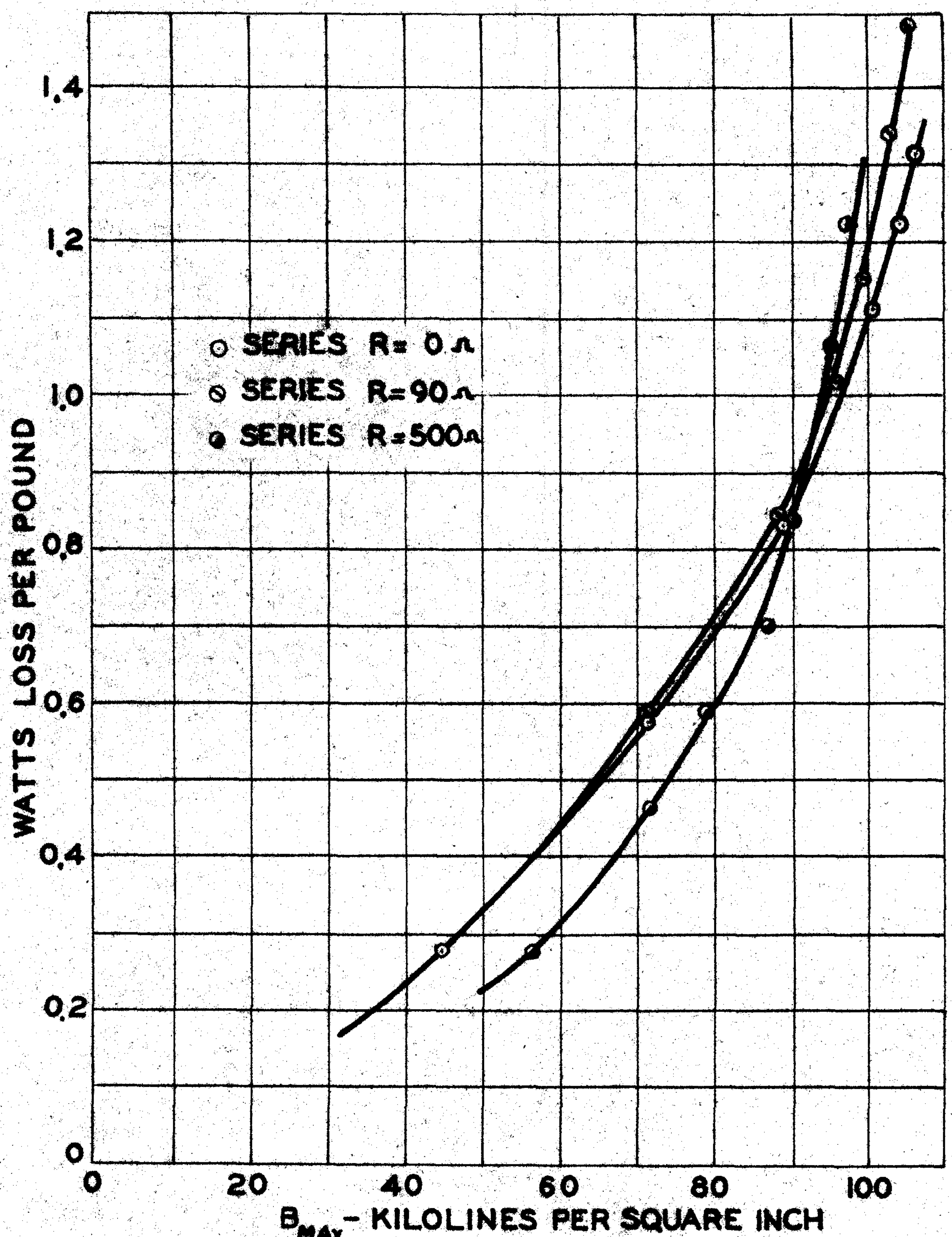

Fig. 13. Variation of Iron Losses with Waveform of the Applied Voltage.

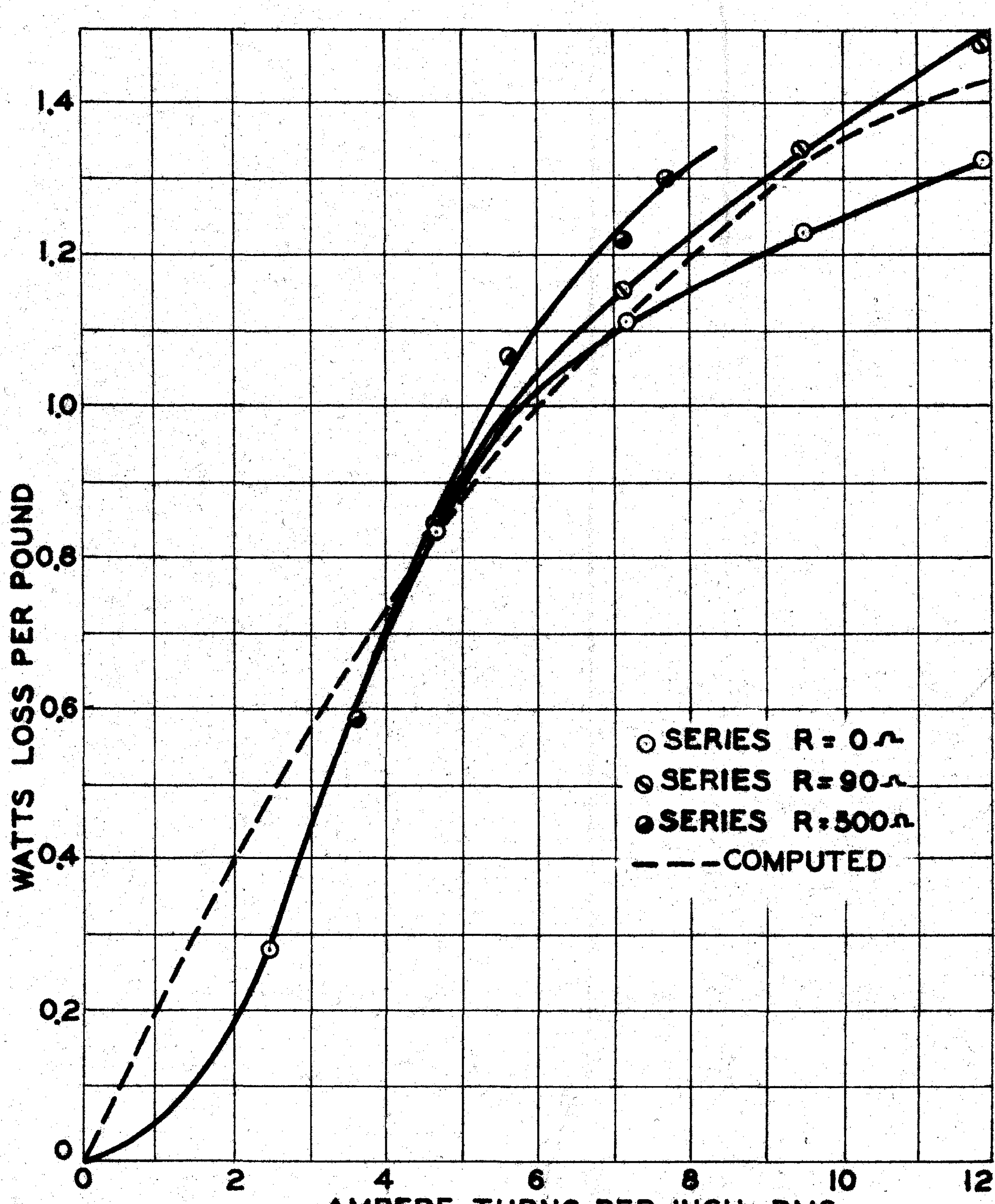

Fig. 14. Variation of Iron Losses with Applied Voltage Waveform.

TABLE 14

Iron Losses Per Pound vs. Maximum Flux Density

Reactor #1, Hipersil Core, Weight 6.9 Pounds

R Ohms	I_{rms} amperes	I_{peak} amperes	$\frac{NI_{peak}}{l}$	B_{max}	W/lb. Iron Loss
0	0.20	0.25	3.0	45,000	0.28
"	0.30	0.42	5.0	71,000	0.58
"	0.40	0.65	7.7	89,000	0.83
"	0.50	0.90	10.7	96,800	1.00
"	0.60	1.15	13.7	100,300	1.11
"	0.80	1.65	19.5	104,000	1.23
"	1.00	2.16	25.6	106,200	1.32
90	0.20	0.25	3.0	45,000	0.28
"	0.30	0.42	5.0	71,000	0.59
"	0.40	0.63	7.5	88,700	0.84
"	0.50	0.87	10.3	96,000	1.01
"	0.60	1.09	12.9	99,400	1.15
"	0.80	1.52	18.0	103,300	1.34
"	1.00	1.90	22.5	105,000	1.49
500	0.20	0.32	3.8	57,000	0.28
"	0.25	0.42	5.0	71,000	0.46
"	0.30	0.50	5.9	79,000	0.59
"	0.35	0.62	7.3	88,000	0.70
"	0.40	0.66	7.8	90,000	0.84
"	0.50	0.81	9.6	95,000	1.07
"	0.60	0.96	11.4	97,600	1.22

on Hipersil steel then is:

$$R_e/lb = \frac{0.213\ N}{l I} - \frac{0.00784\ N^2}{l^2} \qquad (54)$$

TABLE 15

Iron Losses Per Pound vs. RMS Ampere Turns Per Inch

Reactor #1 - Hipersil Core, Weight 6.9 Pounds

R Ohms	$\frac{NI_{rms}}{l}$	W/lb. Iron Loss
0	2.4	0.28
"	4.7	0.83
"	7.1	1.11
"	9.5	1.23
"	11.9	1.32
90	2.4	0.28
"	4.7	0.84
"	7.1	1.15
"	9.5	1.34
"	11.9	1.49
500	2.4	0.28
"	3.6	0.59
"	4.7	0.84
"	5.7	1.07
"	7.1	1.22
"	7.7	1.30

TABLE 16

Calculated Iron Loss Per Pound From Equation (53)

$\frac{NI_{rms}}{l}$	W/lb. Iron Loss
2	0.395
4	0.725
6	1.00
8	1.20
10	1.35
12	1.43

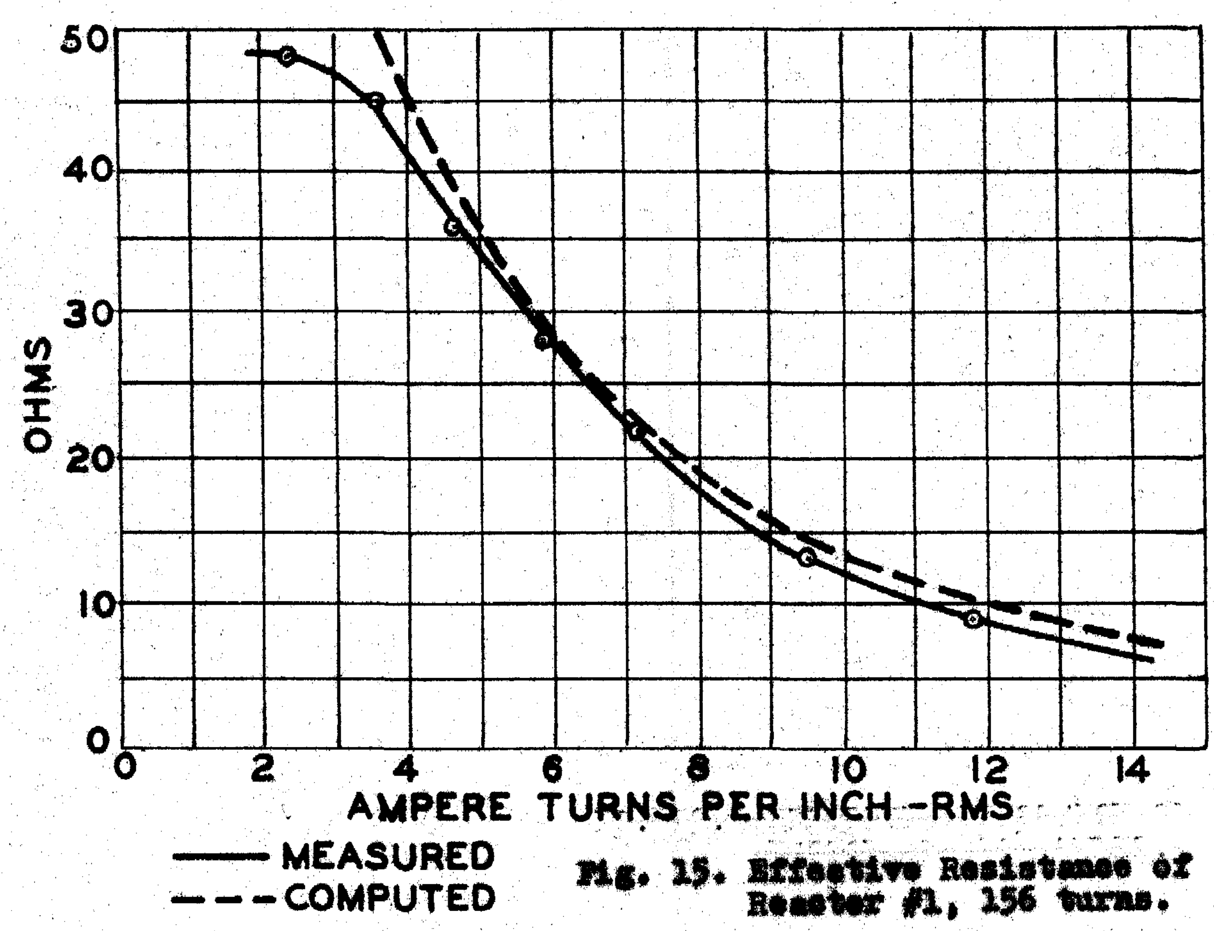

Fig. 15. Effective Resistance of Reactor #1, 156 turns.

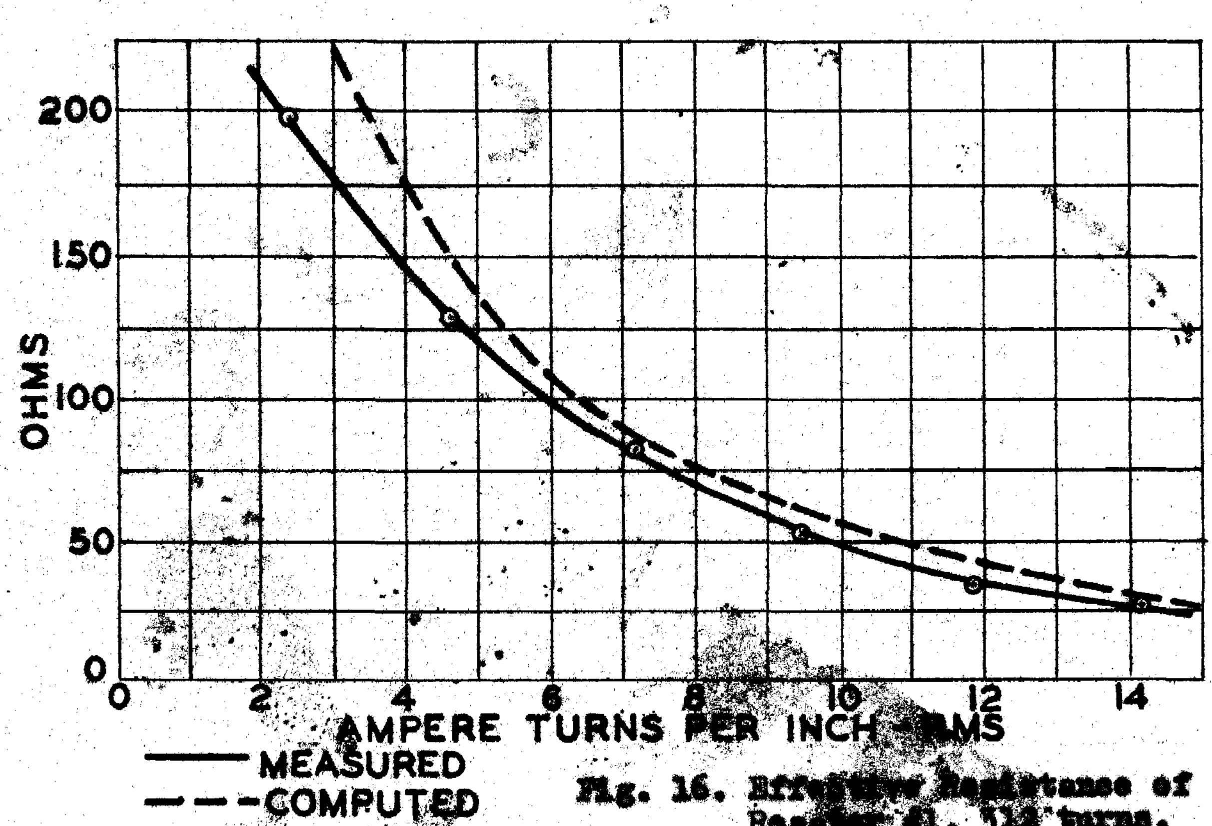

Fig. 16. Effective Resistance of Reactor #1, 312 turns.

An experimental check of equation (54) was obtained by measuring the iron loss of reactor #1, 156 turns, computing the effective resistance by $R_e = W/I^2$ and plotting it as the solid curve on Figure 15, from data in Table 17. The dashed curve was computed from (54), using a weight of 6.9 pounds of iron.

Very close agreement with theory is obtained except at very low magnetizing forces, where the empirical curve is not a good fit for the iron loss curve. This affects only a minor portion of the operating range of the reactor.

TABLE 17

Effective Resistance-Reactor #1 - 156 Turns

Measured and Computed from $R_e = W/I^2$

I_{rms}	$\frac{NI_{rms}}{l}$	W Iron Loss	R_e Ohms
0.2	2.4	1.9	47
0.3	3.6	4.1	46
0.4	4.7	5.8	36
0.5	5.9	7.1	28
0.6	7.1	7.7	22
0.8	9.5	8.6	13
1.0	11.9	9.1	9

To further check equation (54) the work was repeated with a coil of 312 turns on the same core. The results again checked very closely and are shown in Figure 16.

TABLE 18

Effective Resistance-Reactor #1 - 156 Turns

Computed by Equation (54)

$\frac{NI_{rms}}{l}$	R_e Ohms
2	96
4	45
6	28
8	19
10	14
12	10
14	8

TABLE 19

Effective Resistance-Reactor #1 - 312 Turns

Measured and Computed by $R_e = W/I^2$

I_{rms}	$\frac{NI_{rms}}{l}$	W Iron Loss	R_e Ohms
0.1	2.4	2.0	196
0.2	4.7	5.2	129
0.3	7.1	7.5	83
0.4	9.5	8.3	52
0.5	11.9	9.1	36
0.6	14.2	9.5	26

TABLE 20

Effective Resistance-Reactor #1 - 312 Turns

Computed by Equation (54)

$\frac{NI_{rms}}{l}$	R_e Ohms
2	382
4	175
6	108
8	75
10	54
12	40
14	30

D. Ferro-reactance

A discussion of ferro-reactance and of the design of units to give a specified value really hinges on the proof of existence of the weighting factor "k" of equation (47). In other words can a value "k" be found for which

$$X = \omega D \operatorname{sech} \frac{kaNI}{l} \quad \text{ohms} \tag{55}$$

for all values of i?

The effective reactance can be obtained by measurement of impedance and using the relation that:

$$X = \sqrt{Z^2 - R_e^2}$$

where R_e is obtained from $R_e = W/I^2$. The calculated values can be obtained from (55) after finding a value for "k".

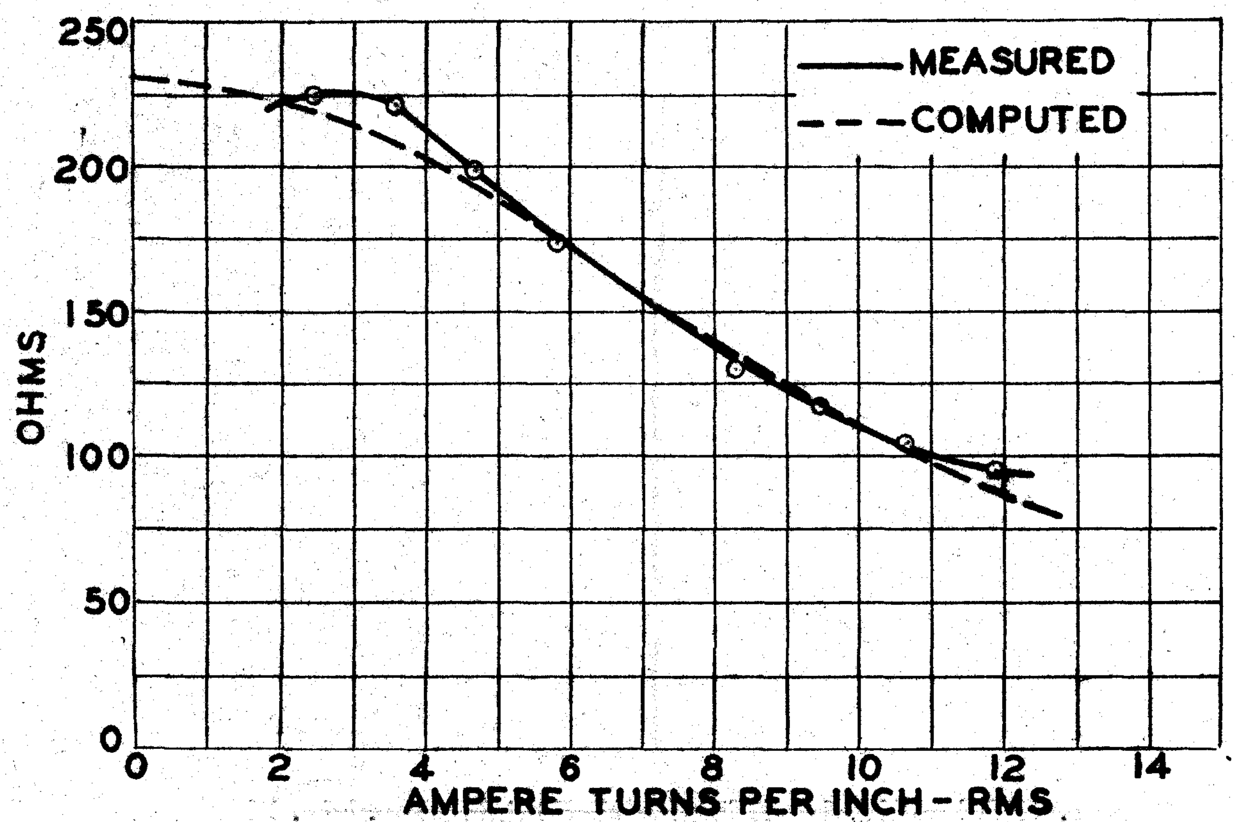

Fig. 17. Reactance of Reactor #1, 156 turns.

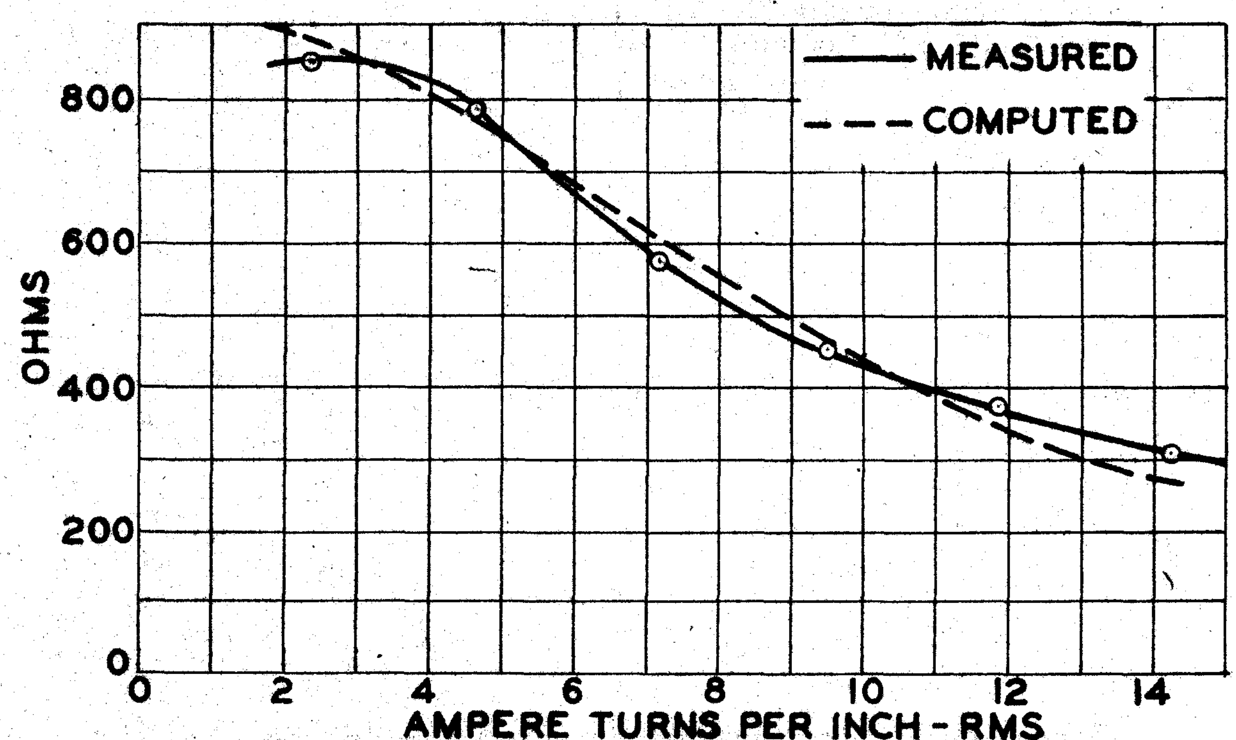

Fig. 18. Reactance of Reactor #1, 312 turns.

TABLE 21

Measured Reactance of Reactor #1 - 156 Turns

Volts	Amperes	$\frac{NI_{rms}}{1}$	W Watts	$R_e = \frac{W}{I^2}$ Ohms	Z Ohms	X Ohms
46.0	0.20	2.4	1.9	47	230	225
68.5	0.30	3.6	4.1	46	228	222
80.5	0.40	4.7	5.8	36	201	198
87.3	0.50	5.9	7.1	28	175	174
90.0	0.60	7.1	7.7	22	150	150
92.0	0.70	8.3	8.3	17	131	131
94.0	0.80	9.5	8.6	13	118	118
95.0	0.90	10.7	8.9	11	105	105
96.2	1.00	11.9	9.1	9	96	96

TABLE 22

Measured Reactance of Reactor #1 - 312 Turns

Volts	Amperes	$\frac{NI_{rms}}{1}$	W Watts	$R_e = \frac{W}{I^2}$	Z Ohms	X Ohms
87	0.10	2.4	2.0	196	870	850
160	0.20	4.7	5.2	129	800	790
175	0.30	7.1	7.5	83	585	578
182	0.40	9.5	8.3	52	455	450
187	0.50	11.9	9.1	36	374	373
189	0.60	14.2	9.5	26	305	305

TABLE 23

Calculated Effective Reactance-Reactor #1 - 156 Turns

$k = 0.5$; $\omega D = 232$

$\frac{NI_{rms}}{l}$	sech $\frac{kaNI}{l}$	X_e Ohms
0	1.000	232
2	0.965	224
4	0.865	201
6	0.738	171
8	0.604	140
10	0.480	111
12	0.364	84

TABLE 24

Calculated Effective Reactance-Reactor #1 - 312 Turns

$k = 0.5$; $\omega D = 928$

$\frac{NI_{rms}}{l}$	sech $\frac{kaNI}{l}$	X_e Ohms
0	1.000	928
2	0.965	896
4	0.870	804
6	0.740	684
8	0.604	560
10	0.482	444
12	0.390	336
14	0.292	271

Tables 21 and 22 give measured values of reactance for reactor #1 with coils of 156 and 312 turns respectively, on the Hipersil core. These values are plotted as solid lines in Figures 17 and 18.

From Figure 17 "k" can now be computed from the measured curve. Arbitrarily choose a point well out on the reactance curve, say at 10 ampere turns per inch, at which point the reactance is 112 ohms. If a value "k" exists then this value of reactance, and all other points on the curve, should be predicted by equation (55):

$$X = \omega D \operatorname{sech} \frac{kaNI}{l} = 112 \qquad \text{at 10 amp.turns/inch.}$$

$$\omega = 377$$

$$D = \frac{aAB_uN^2}{10^8 l} = \frac{0.273 \times 1.87 \times 65000 \times 156^2}{13.15 \times 10^8}$$

$$\omega D = 232$$

$$232 \operatorname{sech} 2.73k = 112$$

$$\operatorname{sech} 2.73k = 0.480$$

From Tables:

$$2.73k = 1.362$$

$$k = 0.50$$

Another check on "k" can be obtained from Figure 18 for the 312 turn coil on the same core. Choose the point at 10 ampere turns per inch at which the reactance is 423 ohms:

$$X = \omega D \operatorname{sech} 2.73k = 423$$

$$\omega D = \frac{377 \times 0.273 \times 1.87 \times 65000 \times 312^2}{13.15 \times 10^8}$$

$$\omega D = 928$$

$$928 \operatorname{sech} 2.73 k = 423$$

$$\operatorname{sech} 2.73 k = 0.456$$

$$2.73 k = 1.420$$

$$k = 0.52$$

Within the limits of experimental accuracy this may be considered 0.5, the same value as obtained for the 156 turn coil. This upholds the assumption that "k" was a function of the iron and not of the turns.

Using "k" as 0.5 and equation (55) the reactance for various values of current is calculated in Table 23 for the 156 turn coil and Table 24 for the 312 turn coil. This data is then plotted as the dashed curves in Figures 17 and 18.

Remarkably close agreement is shown over almost the entire range. This fully substantiates the assumptions behind equation (55) and permits its use to calculate the reactance of a coil for any value of current, or to design a coil to have a particular reactance at a definite rms current value.

To determine somewhat the range of values to be expected for "k", reactors #2 and #3 were built. Magnetization curves were first measured for the steels concerned, since manufacturers' data are unreliable in predicting the performance of an actual core with air gaps unavoidably present. For the magnetization curves empirical equations were calculated and constants for the reactors were as follows:

Reactor #2	Reactor #3
Core: Nicaloi	Core: Silicon steel, analysis unknown.
Turns: 180	Turns: 140
Constants: a - 2.46	Constants: a - 0.604
B_n - 25,300	B_n - 22,700
c - 4,100	c - 1,750
Magnetic length - 7.0 inches	Magnetic length - 10.8 inches
Cross section A - 0.42 sq. in.	Cross section A - 1.52 sq.in.
Constant k - 0.415	Constant k - 0.304

The three reactors used cover a wide range of characteristics, including a high permeability nickel steel, a high quality transformer steel and a very ordinary silicon steel, as well as covering a range of physical sizes as shown in the photographs, Figures 19 and 20. Figure 19 shows the form of split core, with a ground joint, used with the Hipersil core on reactor #1. The other cores are conventional, of E and I punchings.

The data for the measured reactances for reactors #2 and #3 are given in Tables 25 and 26. From this data computations for the value of k were carried out and values of k = 0.415

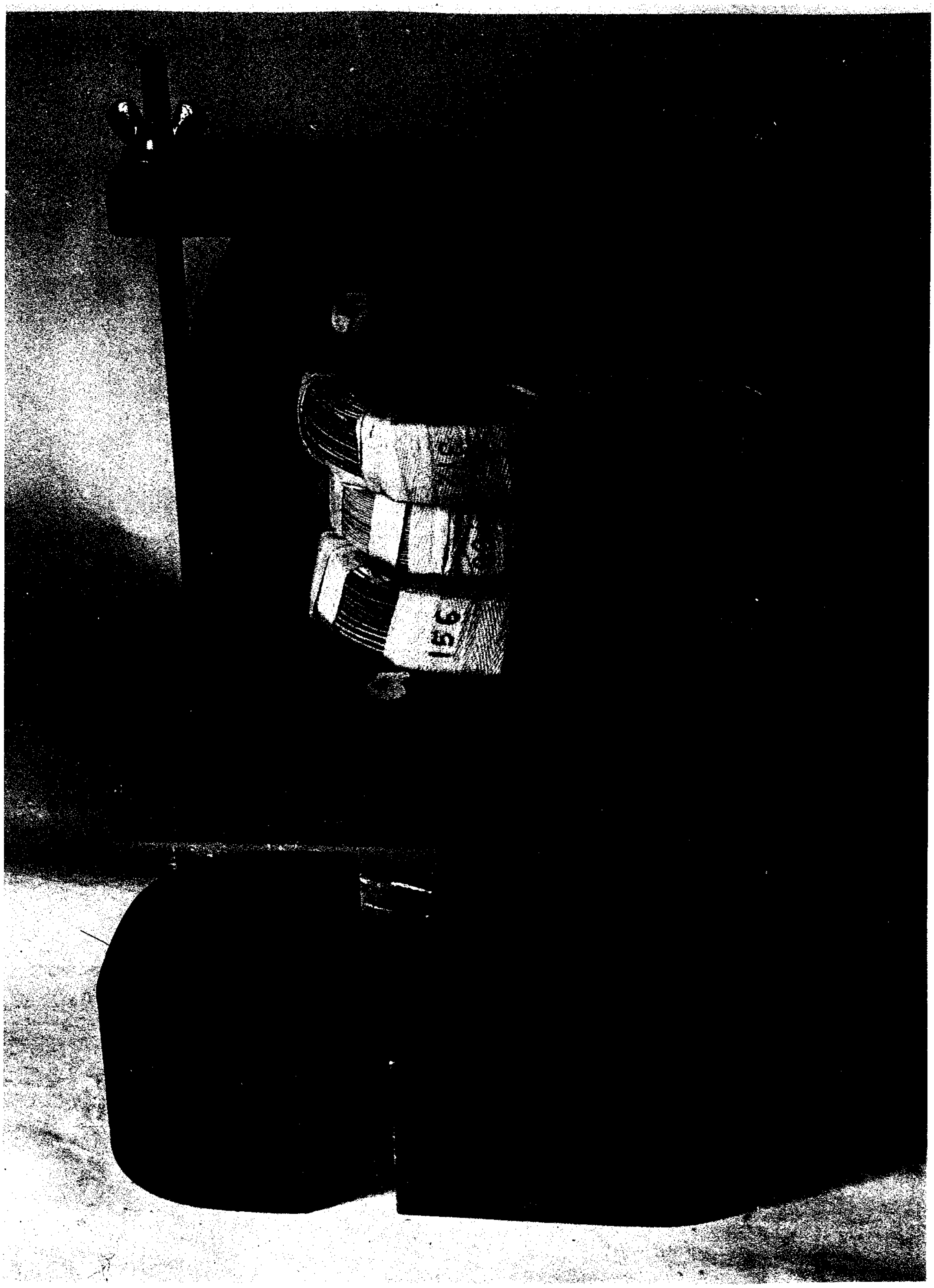

Fig. 19. Reactor #1.

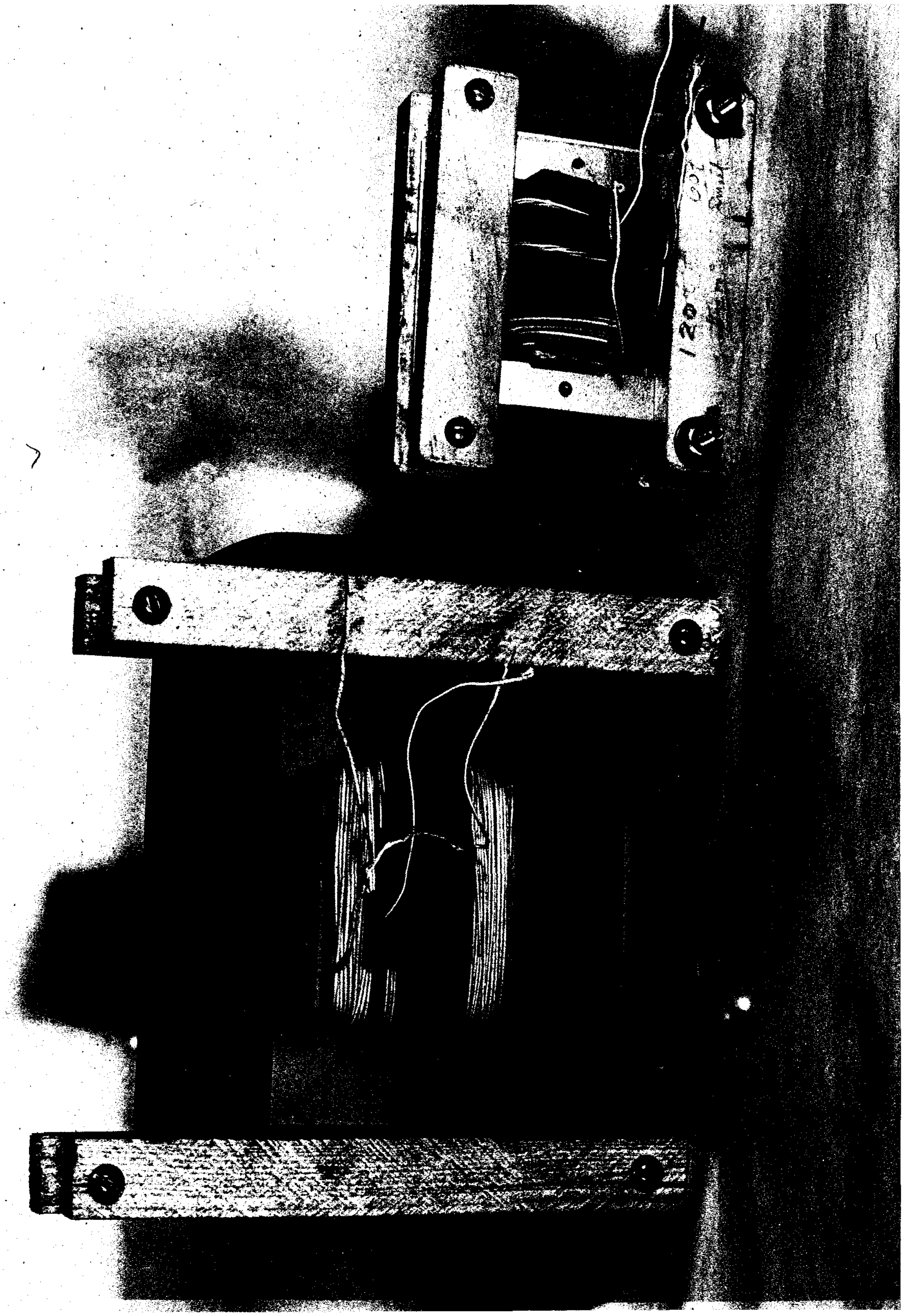

Fig. 20. Left, Reactor #3; Right, Reactor #2.

for reactor #2 and k = 0.304 for reactor #3 were found. This shows that over a wide range of steels, the value of k does not change greatly. Since the magnetization curves were measured with and include the effect of incidental air gaps, the latter factor may be responsible for a considerable part of the change in k.

Using the above values of k the reactances are calculated and shown in Tables 27 and 28. The measured values are then plotted in Figures 21 and 22 as solid lines, and the computed values as dashed lines.

The experimental evidence seems to definitely establish that a factor k does exist as a weighting factor, permitting calculation of the effective reactance in a-c circuits, for any desired value of effective current flowing through the ferro-reactor.

TABLE 25

Measured Reactance-Reactor #2

Nicaloi Core

Volts	Amperes	$\frac{NI_{rms}}{l}$	W Watts	$R_e = \frac{W}{I^2}$ Ohms	Z Ohms	X Ohms
4.3	0.010	0.26	0.03	75	430	425
7.9	0.020	0.51	0.2	125	395	390
10.9	0.040	1.03	0.3	83	273	247
12.5	0.060	1.54	0.4	63	208	191
13.4	0.080	2.06	0.5	50	167	155

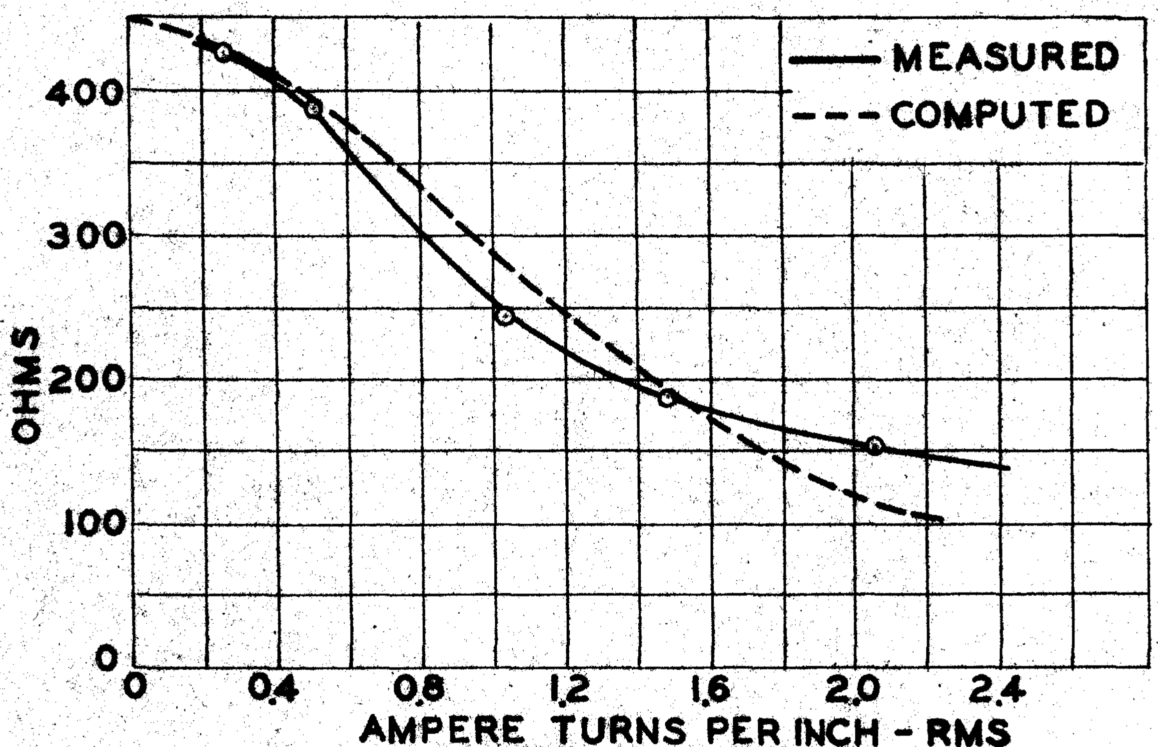

Fig. 21. Reactance of Reactor #2.

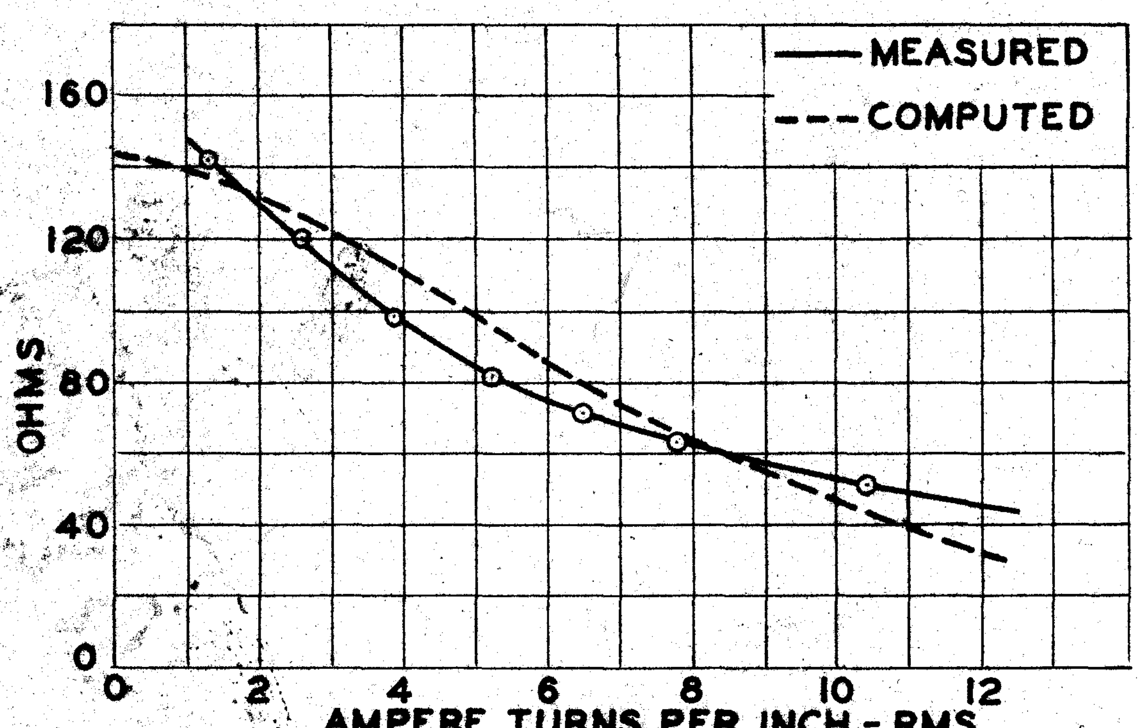

Fig. 22. Reactance of Reactor #3.

TABLE 26

Measured Reactance-Reactor #3

Silicon Steel Core

Volts	Amperes	$\frac{NI_{rms}}{l}$	W Watts	$R_e = \frac{W}{I^2}$ Ohms	Z Ohms	X Ohms
16.0	0.10	1.3	0.8	75	160	141
25.5	0.20	2.6	1.8	45	128	120
31.0	0.30	3.9	2.6	29	103	99
33.8	0.40	5.2	3.3	20	85	82
36.8	0.50	6.5	4.0	16	74	72
38.8	0.60	7.8	4.7	13	65	63
42.6	0.80	10.4	6.2	10	53	52

TABLE 27

Calculated Reactance-Reactor #2

Nicaloi Core, $k = 0.415$, $\omega D = 450$

$\frac{NI_{rms}}{l}$	sech $\frac{kaNI}{l}$	X_e Ohms
0.00	1.00	450
0.20	0.98	440
0.40	0.92	415
0.60	0.84	380
0.80	0.74	334
1.00	0.64	288
1.50	0.41	184
2.00	0.26	117

TABLE 28

Calculated Reactance - Reactor #3

Silicon Steel Core, $k = 0.304, \omega D = 142$

$\frac{NI_{rms}}{l}$	$\operatorname{sech} \frac{kaNI}{l}$	X_e Ohms
0	1.000	142
1	0.982	139
2	0.937	133
4	0.780	111
6	0.600	85
8	0.436	62
10	0.313	45
12	0.219	31

Some argument may be made that these checks have been entirely with applied sinusoidal voltages and that values of k may change when non-sinusoidal voltage is applied as in the case of resistance in series with the reactor, since the current waveform, and consequently the weighting factor may change.

Experimental evidence to satisfactorily refute this point has been secured. The value of k may change but it is usually over such a small range as to make the error introduced less than ten per cent. Data were taken in order to compute the impedance $Z = E/I$ in a series circuit of resistance and ferroreactance. This impedance value was compared with the impedance calculated from:

$$Z = \sqrt{R_e^2 + X_e^2}$$

using (54) and (55) for computing R_e and X_e . The results are tabulated in Table 29 for comparison. Agreement in all cases is better than 8 per cent, the greatest error occurring for the high resistance case, in which the waveform of current was the most nearly sinusoidal. This indicates a need for a slightly modified value of k, but since the error is so small, and since not much further change in waveform could take place, it is felt that the single value of k for the iron in this reactor should be satisfactory for all cases.

TABLE 29

Comparison of Measured and Calculated Impedance

Reactor #1 - 156 Turns

Amperes	Volts	$\frac{NI_{rms}}{l}$	Series R Ohms	R_e Calculated	X_e Calculated	Total R Ohms	Z Calc.	Z Meas.
0.40	77.5	4.7	2	38	192	40	195	194
0.80	93.0	9.5	2	14	118	16	119	116
0.40	93.2	4.7	92	38	192	130	232	233
0.80	132.0	9.5	92	14	118	106	159	165
0.40	223.0	4.7	446	38	192	484	520	558
0.56	300.0	6.5	446	25	164	471	497	536

Consequently it is seen that a method has been developed for the computation of the impedance of a ferro-reactive circuit at any value of effective current, or conversely, a ferro-reactive circuit can be designed to have a desired impedance at a particular current value.

V. THE FERRO-RESONANT CIRCUIT

A. Resonant Voltage

Equation (48) assumes for a series circuit of R, L, and C:

$$I = \frac{E}{\sqrt{R^2 + \left(\omega D \operatorname{sech} \frac{kaNI}{l} - \frac{1}{\omega C}\right)^2}}$$

I and E being rms values. The possibility exists that the second term under the radical may go to zero at some value of I. At this point the denominator is small and the current abruptly increases. A circuit, including a ferro-reactor, in which this happens is said to be ferro-resonant, because of the similarity of the properties to frequency resonance.

Such circuits have assumed considerable importance in the last fifteen years and an analysis for the important circuit properties would be a desirable application and test of the ferro-reactance relations developed.

One of the important circuit values, useful either for design or operation, is the voltage at which the resonant current jump takes place. Since

$$Z = \sqrt{R^2 + \left(\omega D \operatorname{sech} \frac{kaNI}{l} - \frac{1}{\omega C}\right)^2} \quad , \qquad (49)$$

and the usual definition of resonance places the reactive terms equal to zero, then at resonance:

$$\omega D \operatorname{sech} \frac{kaNI_R}{l} = \frac{1}{\omega C}$$

$$\operatorname{sech} \frac{kaNI_R}{l} = \frac{1}{\omega^2 DC}$$

$$\cosh \frac{kaNI_R}{l} = \omega^2 DC$$

$$I_R = \frac{l}{aNk} \cosh^{-1}(\omega^2 DC) \qquad (56)$$

where I_R is the current at resonance. It is not readily possible to measure this current, since before it is reached the current rises to a higher value. The voltage is, however, practically constant through this range and can be readily measured as the resonant voltage E_R of the circuit.

At resonance, since the reactance is zero, the total voltage appears across the circuit resistance. Therefore:

$$E_R = I_R R$$

$$= \frac{Rl}{aNk} \cosh^{-1}(\omega^2 DC) \qquad (57)$$

where R is made up of the circuit resistance plus the effective resistance of the reactor or:

$$R = R_x + R_e \qquad (58)$$

Using reactor #1 in series with a variable resistance and a capacity C, data were taken to check the value of resonant voltage given by equation (57). Table 30 presents these data and Figure 23 is a plot of the results.

TABLE 30

Resonant Voltage vs. Capacity Required

Reactor #1 - 156 Turns

Measured			Computed					
C Mfds.	E_R Volts	R_X Ohms	$\omega^2 DC$	$\cosh^{-1}(\omega^2 DC)$	I_R Amps	R_e Ohms	Total R Ohms	E_R Volts
16.7	39.5	48.5	1.46	0.93	0.58	23	71.5	41
25.0	52.5	48.5	2.18	1.42	0.88	12	60.5	53
41.7	68.5	48.5	3.64	1.97	1.22	7	55.5	68
50.0	73.0	48.5	4.37	2.16	1.34	6	54.5	73

B. Value of Capacity Required for Resonance

Using equation (57):

$$E_R = \frac{Rl}{aNk} \cosh^{-1}(\omega^2 DC)$$

for the resonant voltage with $R = R_x + R_e$, and solving for the value of capacity:

$$\omega^2 DC = \cosh \frac{kaNE_R}{Rl}$$

$$C = \frac{1}{\omega^2 D} \cosh \frac{kaNE_R}{Rl} \quad \text{farads.} \qquad (59)$$

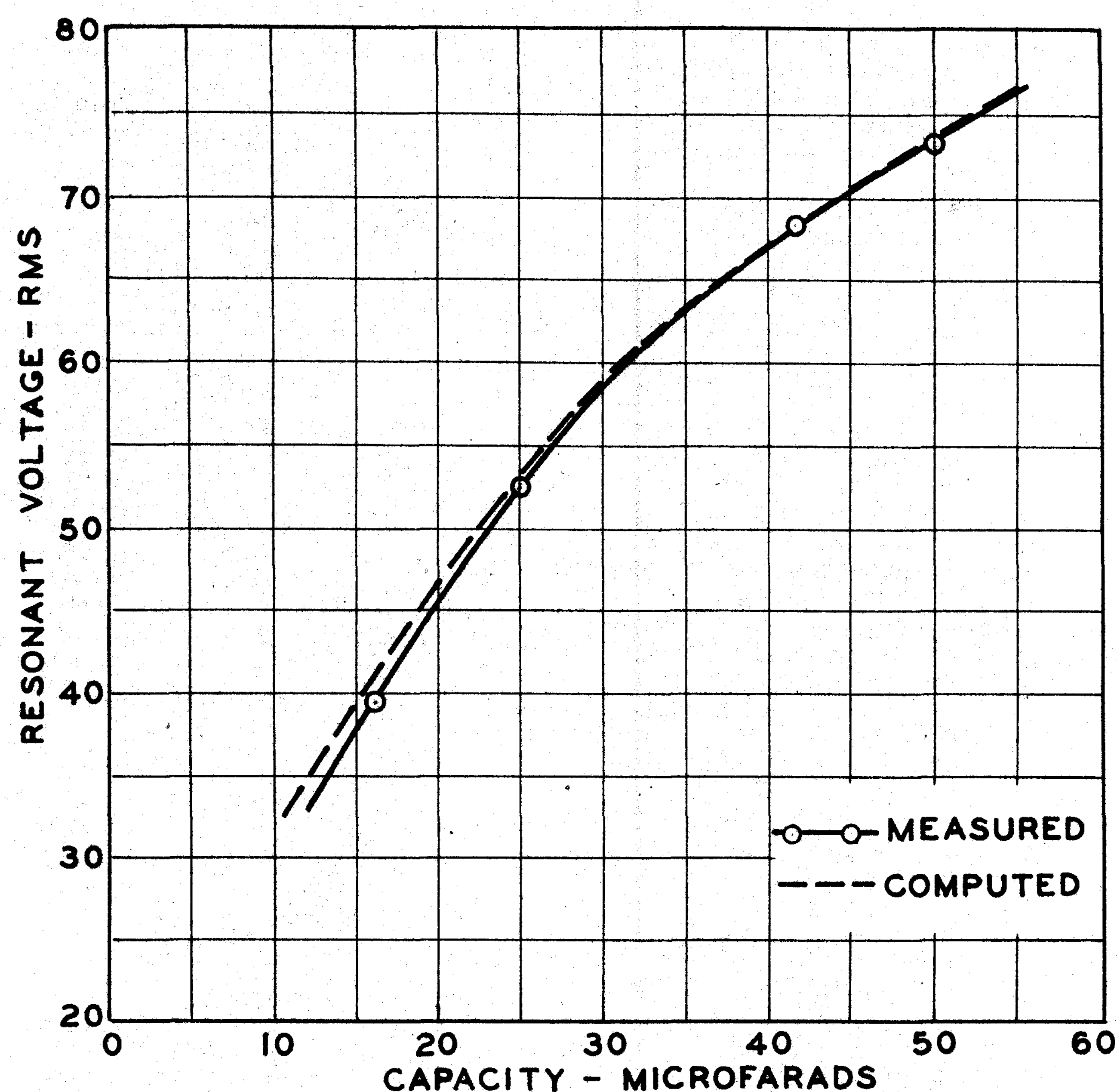

Fig. 23. Value of Capacity Required for Resonance.

This value of capacity will resonate with a reactor having constants D, k, a, N and l in a circuit of total resistance R at a voltage E_R.

C. Circuit Performance

Assume a series circuit using reactor #1, with capacity C of 25 microfarads, and external resistance R_x variable. Equation (49) permits the calculation of the circuit impedance at any value of current. The constants of reactor #1 are:

N - 156 turns

D - 0.614

l - 13.15 inches

A - 1.87 sq.inches

a - 0.273

B_n - 65,000

c - 180 (negligible)

k - 0.5

Figure 24 shows the calculated variation in impedance of this circuit for various values of external circuit resistance R_x. Minimum impedance, actually only the value of the remaining resistance, is reached at resonant current.

Figure 25 is a plot of the computed voltage across the circuit for various values of external resistance. The dashed portions of the curves having negative slope cannot be experimentally realized, as the current jumps directly across on the

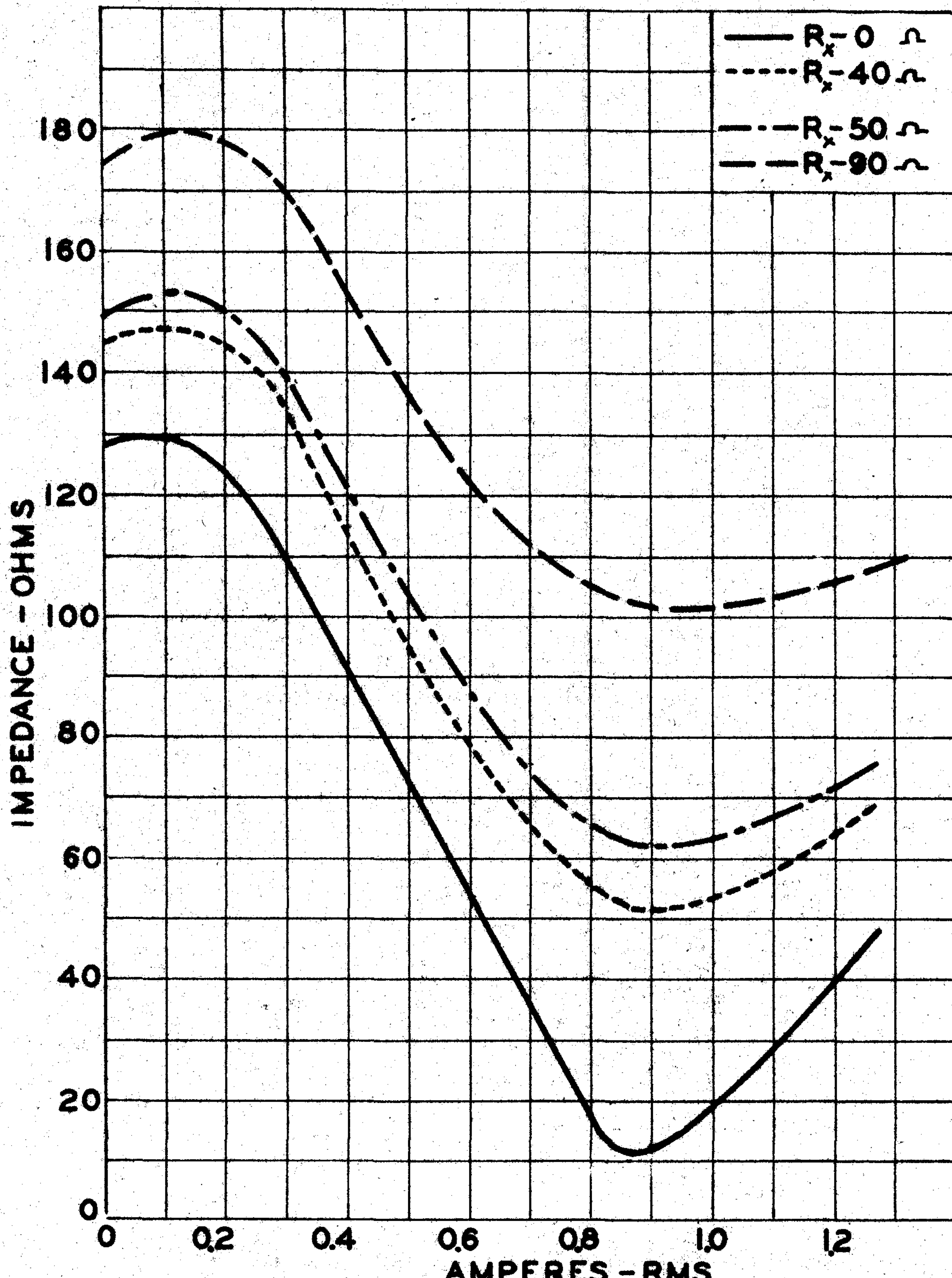

Fig. 24. Impedance of Ferro-resonant Circuit.

path indicated by the arrows. Apparently this jump starts at the point at which the magnitude of the negative rate of change of impedance exceeds the rate of change of current.

As the external resistance in the circuit is increased this jump becomes less, and at some value of resistance the curve of voltage against current has no jump but does have an inflection point, with a single point having a tangent of zero slope. At values of resistance above this the inflection point disappears, as for the curve $R_x = 98$. The curve for $R_x = 50$ has a small jump, so the curve for the inflection point would apparently have external R_x slightly greater than 50 ohms.

For values of small resistance, the jump does not occur at the same value of voltage for increasing as for decreasing voltage. The current in this region is multi-valued. The amount of external resistance which just permits resonance without multi-valued current, or the value producing the curve with a single point of zero slope, is called the critical resistance R_k of the circuit. For many control applications the possibility of two current values is undesirable, so that the value of critical resistance should be known, in order that the external resistance may be kept greater in value than R_k.

Measured values of voltage for various values of external R_x are plotted in Figure 26. There is a very marked agreement, especially in values of voltage at which the current jumps occur, between the measured values of Figure 26 and the totally calculated values of Figure 25.

TABLE 31

Calculated Reactance, Ferro-resonant Circuit

Reactor #1, C- 25 Microfarads

I_{rms} amperes	sech $\frac{kaNI}{l}$	ωD sech $\frac{kaNI}{l}$	X ohms
0.0	1.00	232	126
0.1	0.99	230	124
0.2	0.95	220	114
0.3	0.89	206	100
0.4	0.82	190	84
0.5	0.74	172	66
0.6	0.67	155	49
0.7	0.59	137	31
0.8	0.51	118	12
0.9	0.45	105	-1
1.0	0.39	90	-16
1.2	0.29	67	-39

TABLE 32

Calculated Impedance, Ferro-resonant Circuit

Reactor #1, C = 25 Microfarads

I_{rms} Amps.	X Ohms	R_e Calc.	External R = 0 R Total	Z Ohms	External R = 40 R Total	Z Ohms	External R = 50 R Total	Z Ohms	External R = 98 R Total	Z Ohms
0.0	126	30*	30	129	70	144	80	149	128	178
0.1	124	40*	40	130	80	147	90	153	138	185
0.2	114	48	48	124	88	144	98	154	146	184
0.3	100	47	47	110	87	133	97	139	145	176
0.4	84	38	38	92	78	115	88	121	136	159
0.5	66	28	28	72	68	95	78	102	126	142
0.6	49	22	22	53	62	79	72	87	120	130
0.7	31	18	18	36	58	65	68	75	116	120
0.8	12	14	14	18	54	55	64	65	112	113
0.9	1	12	12	12	52	52	62	62	110	110
1.0	16	10	10	19	50	53	60	62	108	109
1.2	39	9	9	40	49	63	59	71	107	114

* Estimated from circuit data

TABLE 33

Calculated Circuit Voltage, Ferro-resonant Circuit

Reactor #1, C = 25 Microfarads

I_{rms}	External Z	R = 0 E_{rms}	External Z	R = 40 E_{rms}	External Z	R = 50 E_{rms}	External Z	R = 98 E_{rms}
0.00	129	0.0	144	0.0	149	0.0	178	0.0
0.10	130	13.0	147	14.7	153	15.3	185	18.5
0.20	124	24.8	144	28.8	153	30.8	184	36.8
0.30	110	33.0	133	39.9	139	41.7	176	52.8
0.40	92	36.8	115	46.0	121	48.4	159	63.6
0.50	72	36.0	95	49.5	102	51.0	142	71.0
0.60	53	31.8	79	47.4	87	52.2	130	78.0
0.70	36	25.2	65	45.5	75	52.5	120	84.0
0.80	18	14.4	55	44.0	65	52.0	113	90.4
0.90	12	10.8	52	46.8	62	55.8	110	99.0
1.00	19	19.0	53	53.0	62	62.0	109	10.9
1.20	40	48.0	63	75.0	71	85.0	114	13.7

TABLE 34

Measured Circuit Voltage, Ferro-resonant Circuit

Reactor #1, C = 25 Microfarads

External I amps.	R =40 E volts	External I amps.	R =50 E volts	External I amps.	R =68 E volts	External I amps.	R =98 E volts
0.20	34.5	0.20	38.0	0.20	40.0	0.20	43.0
0.30	47.5	0.30	50.5	0.30	53.5	0.30	59.5
0.37	50.5	0.40	54.0	0.40	59.0	0.40	67.5
		0.43	54.5	0.50	60.5	0.50	73.2
0.95	50.0			0.60	62.3	0.60	78.3
1.00	50.5	0.65	54.5	0.70	65.4	0.70	85.3
0.90	47.5	0.70	55.6	0.80	70.0	0.80	93.2
0.80	46.0	0.80	58.0	0.90	75.2	0.90	102.5
		0.90	61.7	1.00	82.5	1.00	113.0
0.29	46.0	1.00	67.2				
0.20	36.0	0.90	62.0				
		0.80	57.5				
		0.70	55.0				
		0.60	53.5				
		0.55	53.3				
		0.39	53.3				
		0.30	50.3				

Analyses were made of several current waveforms in ferro-resonant circuits in the hope of discovering some marked change in harmonic content at resonance, or for values of resistance above and below the critical. These analyses gave no useful information, except that above resonance the third harmonic current was observed as high as fifty six per cent and the total harmonics reached sixty-one per cent.

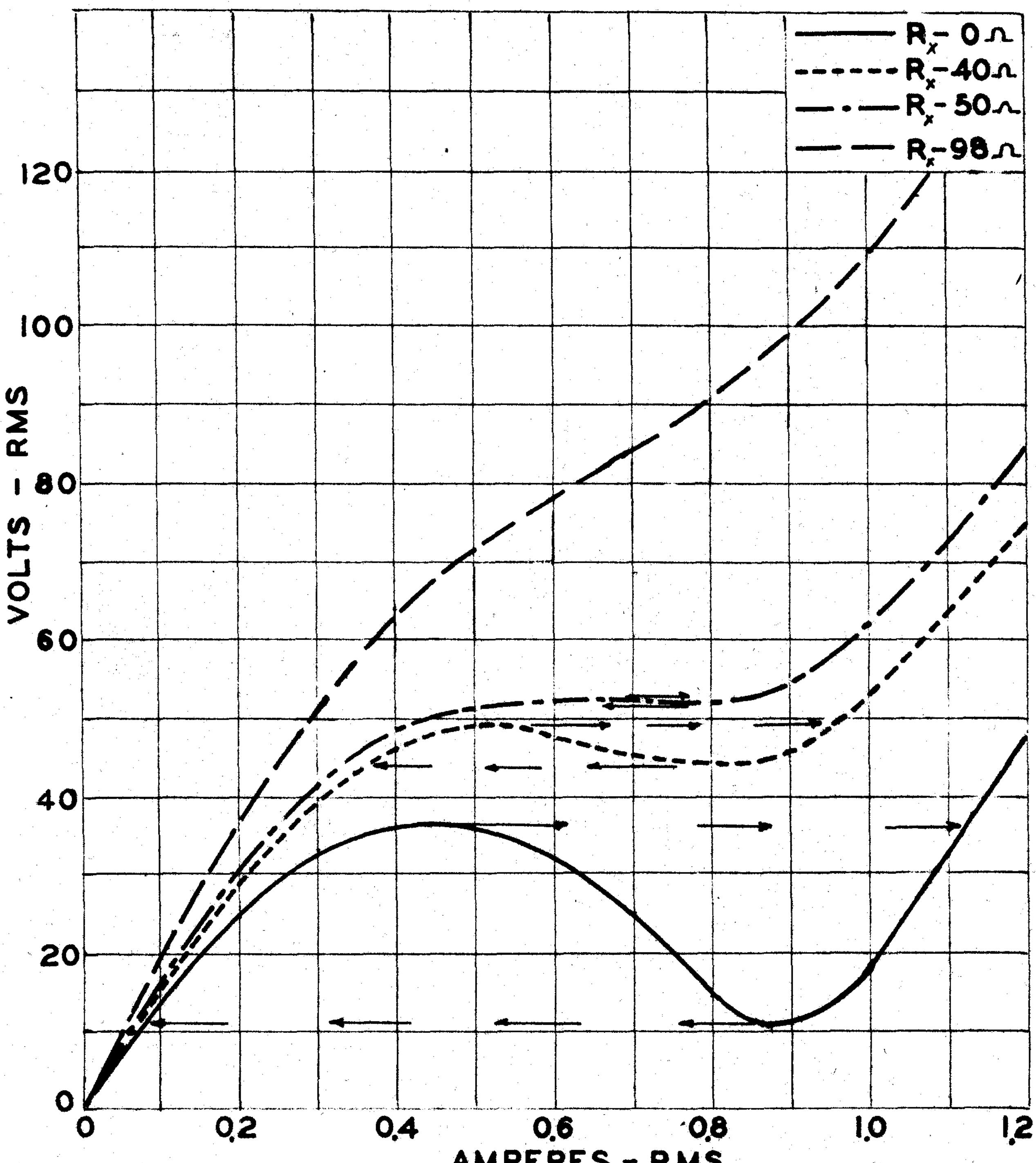

Fig. 25. Calculated Variation of Voltage Across a Ferro-resonant Circuit.

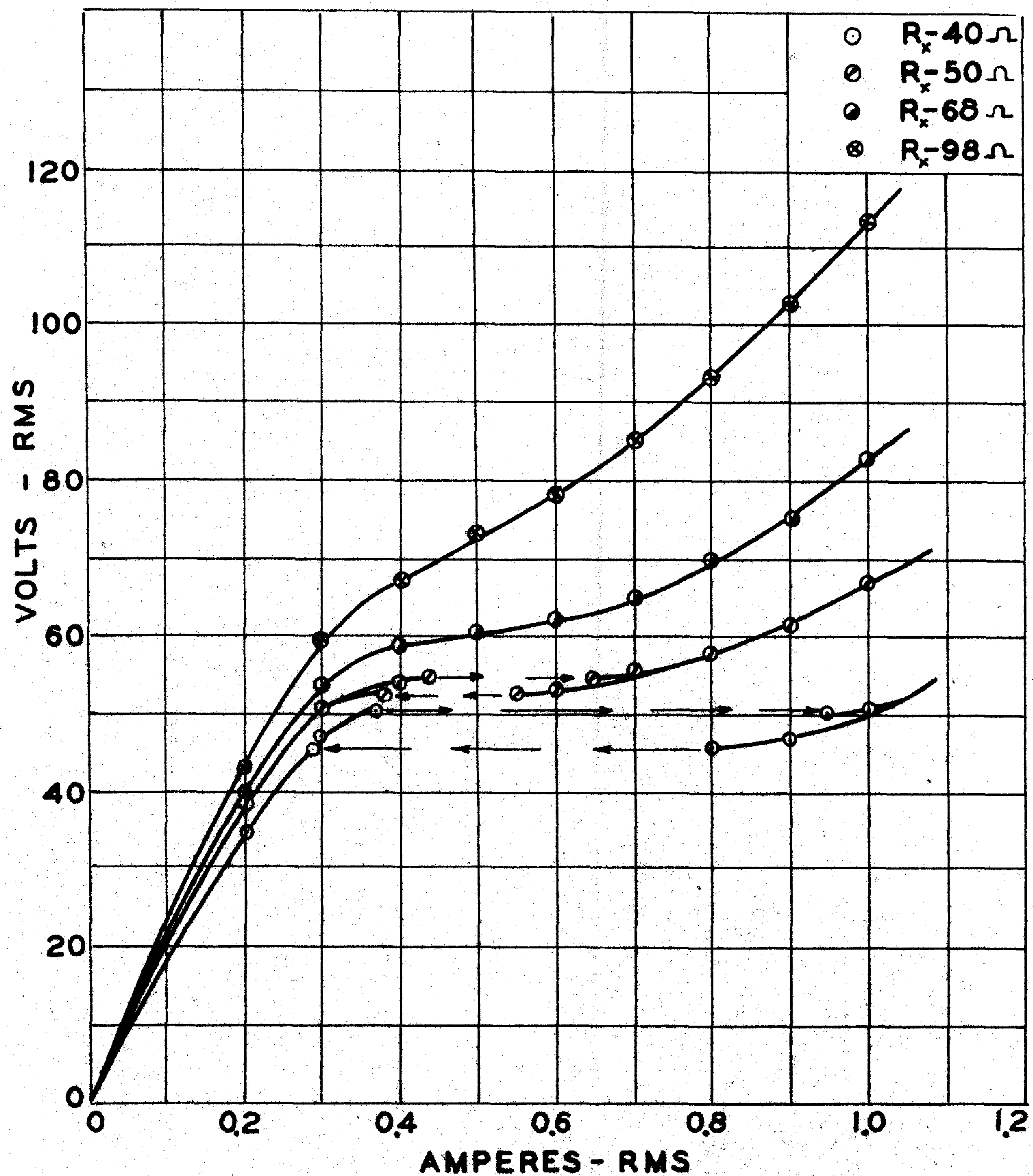

Fig. 26. Measured Variation of Voltage Across a Ferro-resonant Circuit.

D. Value of the Critical Resistance

The critical resistance of a ferro-resonant circuit is that value of external circuit resistance which will produce a volt-ampere relation with a point of inflection with zero slope, and without multi-values for the current. The voltage can be expressed as:

$$E = I\sqrt{R^2 + \left(\omega D \operatorname{sech} \frac{kaNI}{\ell} - \frac{1}{\omega C}\right)^2} \tag{60}$$

and for this curve the point of inflection will have:

$$\frac{dE}{dI} = 0 \tag{61}$$

Before taking the derivative it is necessary to write R as a function of I, since R includes the effective resistance. From (52) the effective resistance is:

$$R_{e/\ell b} = \frac{K_1 N}{\ell I} + \frac{K_2 N^2}{\ell^2}$$

Adding to this the external resistance R_x of the circuit, including the copper resistance of the reactor, and writing reactor weight as w:

$$R = R_x + \frac{K_1 N w}{\ell I} + \frac{K_2 N^2 w}{\ell^2} \tag{62}$$

Lumping the constant terms together as R_o:

$$R = R_o + \frac{K_1 N w}{\ell I} \tag{63}$$

The voltage equation (60) then becomes:

$$E = I\sqrt{\left(R_0 + \frac{k_1 N w}{l I}\right)^2 + \left(\omega D \operatorname{sech}\frac{haNI}{l} - \frac{1}{\omega C}\right)^2} \tag{64}$$

Then applying the condition of (61):

$$0 = \frac{dE}{dI} = \left[\left(R_0 + \frac{k_1 N w}{l I}\right)^2 + \left(\omega D \operatorname{sech}\frac{haNI}{l} - \frac{1}{\omega C}\right)^2\right]^{\frac{1}{2}}$$

$$+ I\left\{\left[\left(R_0 + \frac{k_1 N w}{l I}\right)^2 + \left(\omega D \operatorname{sech}\frac{haNI}{l} - \frac{1}{\omega C}\right)^2\right]^{-\frac{1}{2}}\right.$$

$$\left.\left[\left(R_0 + \frac{k_1 N w}{l I}\right)\left(-\frac{k_1 N w}{l I^2}\right) - \left(\omega D \operatorname{sech}\frac{haNI}{l} - \frac{1}{\omega C}\right)\frac{k\omega DaN}{l}\operatorname{sech}\frac{haNI}{l}\tanh\frac{haNI}{l}\right]\right\}$$

$$\left(R_0 + \frac{k_1 N w}{l I}\right)^2 + \left(\omega D \operatorname{sech}\frac{haNI}{l} - \frac{1}{\omega C}\right)^2$$

$$= I\left[\frac{R_0 k_1 N w}{l I^2} + \frac{k_1 N^2 w^2}{l^2 I^3}\right] + \frac{kI\omega DaN}{l}\operatorname{sech}\frac{haNI}{l}\tanh\frac{haNI}{l}\left(\omega D \operatorname{sech}\frac{haNI}{l} - \frac{1}{\omega C}\right)$$

$$\left(\omega D \operatorname{sech}\frac{haNI}{l} - \frac{1}{\omega C}\right)^2 - \frac{\omega DaNkI}{l}\operatorname{sech}\frac{haNI}{l}\tanh\frac{haNI}{l}\left(\omega D \operatorname{sech}\frac{haNI}{l} - \frac{1}{\omega C}\right)$$

$$+ \left(R_0 + \frac{k_1 N w}{l I}\right)^2 - I\left(\frac{R_0 k_1 N w}{l I^2} + \frac{k_1^2 N^2 w^2}{l^2 I^3}\right) = 0 \tag{65}$$

The last two terms reduce to

$$R_0\left(R_0 + \frac{k_1 N w}{l I}\right)$$

and writing $\frac{aNI}{l} = \alpha$ for simplification:

$$\left(\omega D \operatorname{sech} k\alpha - \frac{1}{\omega C}\right)^2 - \omega D k\alpha \operatorname{sech} k\alpha \tanh k\alpha \left(\omega D \operatorname{sech} k\alpha - \frac{1}{\omega C}\right) + R_0\left(R_0 + \frac{K_1 N \omega}{l I}\right) = 0 \qquad (66)$$

This is a quadratic in the net circuit reactance and therefore has a solution:

$$\left(\omega D \operatorname{sech} k\alpha - \frac{1}{\omega C}\right) = \frac{\omega D k\alpha \operatorname{sech} k\alpha \tanh k\alpha \pm \sqrt{(\omega D k\alpha \operatorname{sech} k\alpha \tanh k\alpha)^2 - 4R_0\left(R_0 + \frac{K_1 N \omega}{l I}\right)}}{2} \qquad (67)$$

This indicates, in general, two values of the reactance for which dE/dI = 0, unless the radical is zero. The curves of Figures 25 and 26 support this. For large R_o the value of the radical is imaginary hence no real values of reactance for dE/dI = 0 are possible. This is illustrated by the curves for 98 and 68 ohms external resistance.

However, for the curve with the point of inflection having dE/dI = 0, the value of the radical must be zero. Applying this condition results in two equations:

$$(\omega D k\alpha \operatorname{sech} k\alpha \tanh k\alpha)^2 = 4R_0\left(R_0 + \frac{K_1 N \omega}{l I}\right)$$

$$\omega D \operatorname{sech} k\alpha - \frac{1}{\omega C} = \frac{\omega D k\alpha}{2} \operatorname{sech} k\alpha \tanh k\alpha$$

These equations can be put into terms of sinh and cosh:

$$\left(\omega D \frac{k\alpha \sinh k\alpha}{\cosh^2 k\alpha}\right)^2 = 4 R_0 \left(R_0 + \frac{K_1 N_w}{\ell I}\right) \qquad (68)$$

$$\omega D \operatorname{sech} k\alpha - \frac{1}{\omega C} = \frac{\omega D}{2} \frac{k\alpha \sinh k\alpha}{\cosh^2 k\alpha} \qquad (69)$$

Substitute (68) into (69):

$$\omega D \operatorname{sech} k\alpha - \frac{1}{\omega C} = \sqrt{R_0^2 + \frac{R_0 K_1 N_w}{\ell I}}$$

$$= R_0 \sqrt{1 + \frac{K_1 N_w}{\ell I R_0}} \qquad (70)$$

Equation (70) states that at this point the reactance is a function of the circuit resistance. For usual circuit values, dE/dI is zero practically at the point at which the circuit reactance equals the fixed resistance R_0.

Returning to (69):

$$\omega D \operatorname{sech} k\alpha - \frac{1}{\omega C} = \frac{\omega D}{2} \frac{k\alpha \sinh k\alpha}{\cosh^2 k\alpha} \qquad (69)$$

$$\frac{2}{\omega^2 DC} = 2 \operatorname{sech} k\alpha - \frac{k\alpha \sinh k\alpha}{\cosh^2 k\alpha}$$

$$\frac{2}{\omega^2 DC} = \frac{2 \cosh k\alpha - k\alpha \sinh k\alpha}{\cosh^2 k\alpha} \qquad (71)$$

The left hand side of this equation is calculable from circuit constants. Figure 27 is a plot of the function:

$$\frac{2 \cosh k\alpha - k\alpha \sinh k\alpha}{\cosh^2 k\alpha}$$

against values of $k\alpha$. By computing the left side of (71),

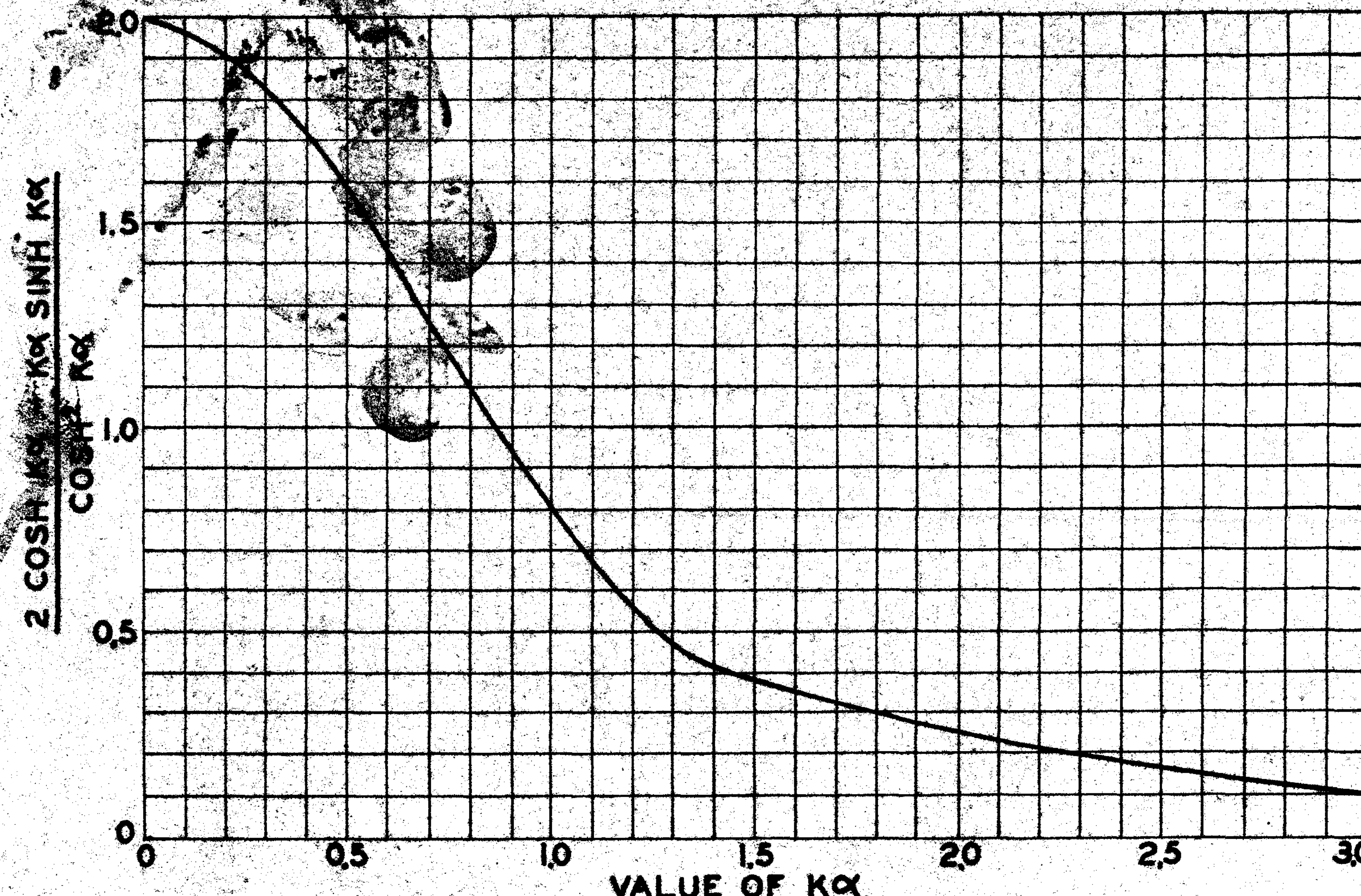

Fig. 27. Variation of [illegible] Kα-Kαsinh Kα

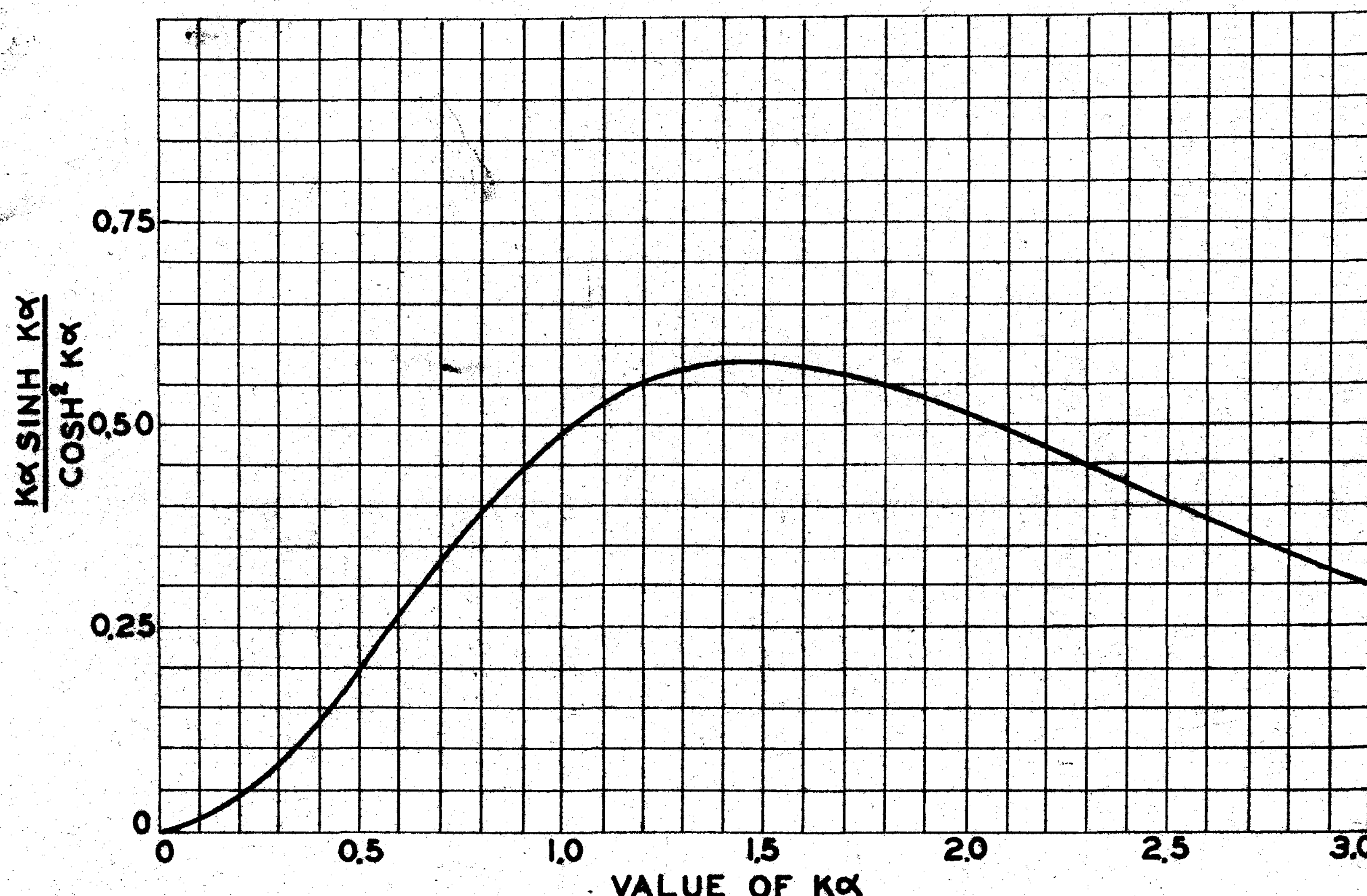

Fig. 28. Variation of $\frac{K\alpha \sinh K\alpha}{\cosh^2 K\alpha}$

entering the curve at the value obtained for the above function, the value of $k\alpha$ may be read from the curve.

The value of I may be secured from $k\alpha$ by a knowledge of the constants of the iron

$$I = \frac{(k\alpha)\,l}{aNk} \tag{72}$$

From (68):

$$\left(\omega D \frac{k\alpha \sinh k\alpha}{\cosh^2 k\alpha}\right)^2 = 4R_0\left(R_0 + \frac{K_1 N w}{lI}\right)$$

may be written:

$$R_0^2 + \frac{K_1 N R_0 w}{lI} - \frac{1}{4}\left(\omega D \frac{k\alpha \sinh k\alpha}{\cosh^2 k\alpha}\right)^2 = 0 \tag{73}$$

and this may be solved as a quadratic:

$$R_0 = \frac{-\dfrac{K_1 N w}{lI} \pm \sqrt{\left(\dfrac{K_1 N w}{lI}\right)^2 + \left(\omega D \dfrac{k\alpha \sinh k\alpha}{\cosh^2 k\alpha}\right)^2}}{2} \tag{74}$$

As shown below, (74) for practical problems will reduce to:

$$R_0 = \frac{\omega D}{2} \frac{k\alpha \sinh k\alpha}{\cosh^2 k\alpha} \tag{75}$$

Figure 28 is a plot of the function:

$$\frac{k\alpha \sinh k\alpha}{\cosh^2 k\alpha} \tag{76}$$

against $k\alpha$. From the value of $k\alpha$ obtained above, and the value of I from equation (72) the value of R_0 may be determined.

TABLE 35

The Functions $\frac{2 \cosh k\alpha - k\alpha \sinh k\alpha}{\cosh^2 k\alpha}$ and $\frac{k\alpha \sinh k\alpha}{\cosh^2 k\alpha}$

$k\alpha$	$\cosh k\alpha$	$\sinh k\alpha$	$\frac{k\alpha \sinh k\alpha}{\cosh^2 k\alpha}$	$\frac{2 \cosh k\alpha - k\alpha \sinh k\alpha}{\cosh^2 k\alpha}$
0.00	1.000	0.000	0.000	2.000
0.32	1.052	0.326	0.095	1.805
0.64	1.220	0.685	0.294	1.358
0.80	1.340	0.888	0.395	1.095
0.96	1.500	1.114	0.476	0.858
1.12	1.696	1.369	0.531	0.646
1.28	1.937	1.659	0.565	0.465
1.60	2.578	2.376	0.572	0.358
1.92	3.484	3.337	0.528	0.275
2.24	4.750	4.643	0.459	0.205
2.88	8.935	8.879	0.322	0.112

The value of external circuit R_x is then found from:

$$R_x = R_o - R_c - \frac{K_2 N^2 w}{\ell^2}$$

Values larger than this must be used in the ferro-resonant circuit to insure single-valuedness for the current.

The value of R_k may be calculated for the circuit previously used, consisting of reactor #1 and a capacity of 25 microfarads. For equation (71):

$$\frac{2}{\omega^2 DC} = \frac{2}{377^2 \times 0.614 \times 25 \times 10^{-6}}$$

$$= 0.918$$

By use of Figure 27 the value of $k\alpha$ is found to be 0.92 from which by equation (72) the current at the inflection point is found to be:

$$I = \frac{0.918 \times 13.15}{0.5 \times 0.273 \times 156}$$

$$= 0.572 \quad \text{amperes}$$

Use of Figure 28 yields for $k\alpha$ = 0.92, a value for the function

$$\frac{k\alpha \sinh k\alpha}{\cosh^2 k\alpha}$$

of 0.51. Then equation (74) results in:

$$R_0 = \frac{-\frac{0.213 \times 156 \times 6.9}{13.15 \times 0.572} \pm \sqrt{\left(\frac{0.213 \times 156 \times 6.9}{13.15 \times 0.572}\right)^2 + \left(232 \times 0.51\right)^2}}{2}$$

$$= \frac{-30.4 \pm \sqrt{900 + 13900}}{2}$$

Since the negative sign has no significance and all the terms are negligible except the term 13900:

$$R_0 = \frac{118}{2} = 59 \quad \text{ohms}$$

The external R_x to be used in the circuit is, for a circuit copper resistance of 8 ohms:

$$R_x = 59 - 8 - \frac{(-0.00784)\, 156^2 \times 6.9}{13.15^2}$$

$$R_x = 58.2 \quad \text{ohms.}$$

Or, more directly by use of (75) and Figure (28), with $k\alpha = 0.92$, and $\omega D = 232$,

$$R_0 = \frac{232 \times 0.51}{2} = 59 \text{ ohms}$$

$$R_x = 58.2 \text{ ohms as before}$$

By reference to Figures 25 and 26 it can be seen that a curve for R equal to 58 ohms would give a curve very close to the correct location for the curve with the inflection point having zero slope. This substantiates the theory developed in this and preceding sections.

VI. VALIDITY OF THE CONSTANT INDUCTANCE ASSUMPTION

As mentioned in the introduction, it has been customary for many years to assume ferro-inductance a circuit constant, and the ferro-reactive voltage drop in a-c circuits as proportional to the current as in:

$$E_m \sin(\omega t + \theta) = \omega L_e I_m \sin \omega t$$

A definition for inductance when using effective current and voltage is usually obtained from:

$$E_L = \omega L_e I$$

or

$$L_e = \frac{E_L}{\omega I} \tag{77}$$

These equations are obviously impossible if inductance is considered a function of current and therefore of time, as actually occurs in an a-c circuit. Equation (77) also requires inductance to be a function of frequency, which does not agree with the usual physical concepts of inductance. A linear voltage-current relation for a ferro-reactor is implied in (77) and such a relation is freely used in the calculation of many a-c circuits containing ferro-reactors without regard to the truth of the implication. It is now possible to determine why and to what extent the assumption of constant L can be supported.

If:

$$X = \omega D \operatorname{sech} k\alpha \quad \text{where} \quad \alpha = \frac{aNI}{l}$$

then the ferro-reactive voltage drop may be written as:

$$E_L = \omega D I \operatorname{sech} k\alpha = \frac{\omega a A B_m N^2 I}{10^8 l} \operatorname{sech} k\alpha$$

$$= \frac{\omega A B_m N}{10^8 k} \frac{k\alpha}{\cosh k\alpha} \qquad (78)$$

The ferro-reactive voltage drop is seen to be a function of $k\alpha/\cosh k\alpha$ and this function is plotted against $k\alpha$ in Figure 29. The value of the function rises in an almost linear manner to a maximum followed by a gradual fall. If an inductor is operated on the lower portion of the rise, then the voltage drop is approximately a linear function of the current, as assumed. The magnitude of departure from linearity can be readily estimated from the curve of this function.

If (78) is written in terms of instantaneous current, by replacing kI by i, the cause of the peaked currents present in strongly excited ferro-inductors is seen in this curve. As the instantaneous voltage applied to an R-L series circuit is increased, the voltage across the reactance fails to increase as rapidly as the source voltage. Consequently the iR voltage drop must increase faster than the increase in source voltage, but this can happen only if the current increases faster than the source voltage. This results in a current peak.

An experimental check of equation (78) was possible with data taken from Table 21 for reactor #1. From this data, the reactive voltage can be obtained by use of:

$$IX = I\sqrt{Z^2 - R_e^2} \qquad (79)$$

and is plotted as the solid line of Figure 30. The reactive voltage drop calculated from equation (78) is presented as the dashed line of this figure and good agreement with the theory is shown over most of the range.

Equation (79) is an expression of Kirchkoff's law, using I as the effective value of a sine wave equivalent in effective value to the distorted wave present. This use of I is an approximation which becomes seriously in error for high harmonic percentages, such as occur for operation over the peak of Figure 29. The lack of agreement between measured and calculated reactor voltages at the higher values of Figure 30 may well be due to the use of I as an equivalent sine wave current, in calculating IX from (79).

Up to values of about five ampere turns rms per inch, the assumption of linear reactive drop is not difficult to support. By reference to Figure 2, it can be seen that five ampere turns rms per inch would place the peak of the magnetomotive force wave below the knee of the magnetization curve. If greater magnetizing forces are used, the assumption of constant L becomes difficult to support.

It has been assumed and experimentally supported that:

$$X = \omega D \operatorname{sech} \frac{kaNI}{l}$$

and then:

$$E_L = IX = \omega DI \operatorname{sech} \frac{kaNI}{l}$$

By (77)

$$L_e = \frac{E_L}{\omega I} = \frac{\omega DI \operatorname{sech} \frac{kaNI}{l}}{\omega I}$$

Then for effective values of current and voltage

$$L_e = D \operatorname{sech} \frac{kaNI}{l} \tag{80}$$

However from (25) for instantaneous current values.

$$L = D \operatorname{sech} \frac{aNi'}{l} \tag{81}$$

For zero current these expressions become equal to D and for reactor #1 D has a value of .614 henry.

If (77) were assumed to hold, then L_e would be the slope of the volt-ampere curve. An approximate value of L_e obtained from the average slope of the linear portion of Figure 30 gives for reactor #1:

$$L_e = \frac{E}{\omega I} = \frac{100}{377 \times 0.45} = 0.59 \quad \text{henrys}$$

This value for L_e checks well the theoretical value of 0.614 henrys obtained for this reactor from (25).

Since L_e involves rms current and L instantaneous current there will be no agreement between the two inductances except at zero current. The comparison of the expressions does, however, show the place of the factor k in the weighted average arrived at over a current cycle with a certain value of rms current flowing.

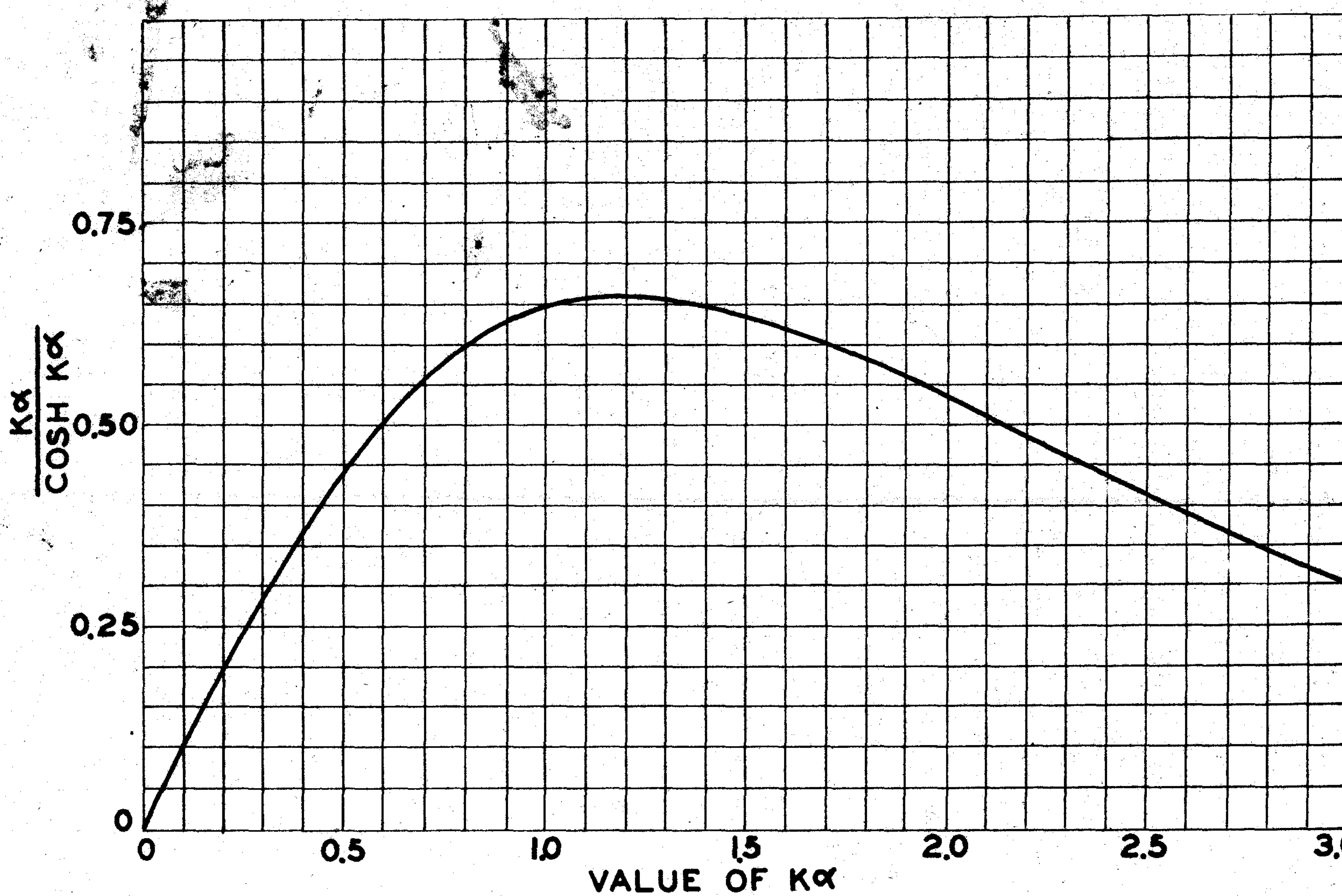

Fig. 29. Variation of $\frac{K\alpha}{\cosh K\alpha}$

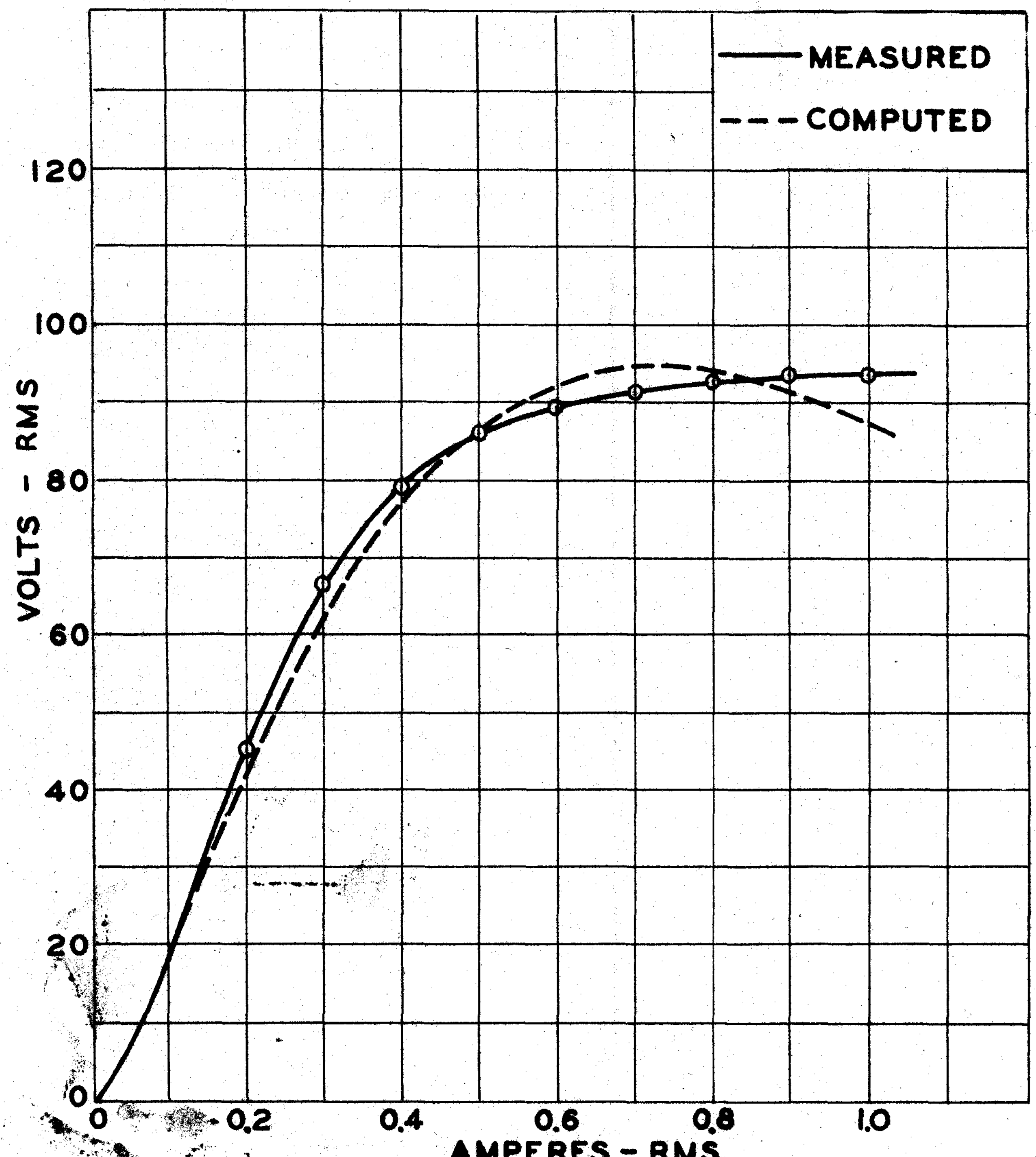

Fig. 30. Voltage Across a Pure Reactance. Reactor #1, 156 turns.

TABLE 36

The Function $\frac{k\alpha}{\cosh k\alpha}$

$k\alpha$	$\cosh k\alpha$	$\frac{k\alpha}{\cosh k\alpha}$
0.00	1.000	0.000
0.32	1.052	0.304
0.64	1.220	0.525
0.80	1.340	0.597
0.96	1.500	0.640
1.12	1.696	0.660
1.28	1.937	0.661
1.60	2.578	0.622
1.92	3.484	0.551
2.24	4.750	0.471
2.88	8.935	0.322

TABLE 37

Reactive Voltage Drop, Reactor #1 - 156 Turns

Computed (77)		Measured *					
I amps.	IX_e volts	I amps.	$\frac{NI}{l}$	E volts	Z ohms	R_e ohms	IX volts
0.17	37.4	0.20	2.4	46.0	230	50	45
0.34	67.7	0.30	3.6	68.5	228	48	67
0.51	86.5	0.40	4.7	80.5	201	39	79
0.67	94.2	0.50	5.9	87.3	175	31	86
0.84	93.6	0.60	7.1	90.0	150	24	89
1.01	88.0	0.70	8.3	92.0	131	19	91
1.18	79.4	0.80	9.5	94.0	118	16	93
		0.90	10.7	95.0	105	13	94
		1.00	11.9	96.2	96	11	94

* Data from Table 21.

VII. SUMMARY

The field of ferro-inductance has been much neglected for many years. This investigation was instituted in an attempt to develop methods which would make ferro-inductive circuits as susceptible of analysis as circuits with constant parameters.

The work has led to the development of an accurate empirical equation for the magnetization curve of a steel. This equation has been applied in predicting the inductance of a ferro-inductor at any value of current, and methods have been developed for the measurement of this inductance, these methods checking the theory closely.

The equation for ferro-inductance has been generalized into a relation for effective ferro-reactance by an assumption, and experimental evidence has been obtained to support the validity of the assumption. Methods were also developed for calculating the effective resistance of an iron-cored reactor. Application was then made of both of these developments in calculating the impedance of circuits containing ferro-reactors, and the results were again well supported by experimental evidence. The latter calculations have apparently never been possible before.

Another application of ferro-reactance was made to the ferro-resonant circuit, and simple relations for resonant voltage, capacity required, and the value of the critical resistance developed. These were all checked by experiment to a satisfactory degree of accuracy. Analytic methods for these solutions were not previously available in simple form.

VIII. SELECTED REFERENCES

1. Barton, J. P. Empirical Equation for the Magnetization Curve. Trans. AIEE v 52 1933 p 659-664.

2. Becker, G. F. and Van Orstrand, C. E. Hyperbolic Functions. Smithsonian Mathematical Tables. Washington, D. C., Smithsonian Institution, 1931.

3. Boyajian, A. Mathematical Analysis of Non-linear Circuits. G. E. Review v 34 1931 p 531-537, 745-751.

4. Charlton, O. E. and Jackson, J. E. Losses in Iron Under Action of Superimposed A-C and D-C Excitation. Trans. AIEE v 44 1925 p 824- 829.

5. Gokhale, S. L. Law of Magnetization. Trans. AIEE v 45 1926 p 1013- 1031.

6. Granville, W. A., Smith, P. F., Longley, W. R. Elements of the Differential and Integral Calculus. Rev. Ed. p 435. New York, Ginn and Co., 1941.

7. Hanna, C. R. Design of Reactances and Transformers Which Carry D-C. Trans. AIEE v 46 1927 p 155-158.

8. Keller, E. G. Beat Theory of Non-linear Circuits. J. Frank. Inst. v 228 1939 p 319-337.

9. --------. Resonance Theory of Series Non-linear Circuits. J. Frank. Inst. v 225 1938 p 561- 577.

10. Lamson, H. W. A Method of Measuring the Magnetic Properties of Small Samples of Transformer Laminations. Proc. IRE v 28 1940 p 541-548.

11. Lippelt, H. The Magnetic Hysteresis Curve. Trans. AIEE v 45 1926 p 395-410.

12. Martienssen, O. Über Neue Resonanzerscheinungen in Wechselstromkreisen. Phys. Zeit. v 11 1910 p 448-460.

13. Odessy, P.D. and Weber, E. Critical Conditions in Ferro-resonance. Trans. AIEE v 57 1938 p 423-431.

14. Rader, L.T. and Litscher, E.G. Some Aspects of Inductance When Iron is Present. Trans. AIEE v 63 1944 p 133-139.

15. Ryan, F.C. Status of Frequency Doublers in Radio Practice. Proc. IRE. v 8 1920 p 509-524.

16. Sanford, R.L. Magnetic Reluctivity Relationship. U.S. Bur. Stds. Sci. Paper v 21 1926 p 743-755.

17. Suits, C.G. Studies in Non-linear Circuits. Trans. AIEE v 50 1931 p 724-736.

18. --------. A Voltage Selective Non-linear Bridge. Physics v 1 1931 p 171-181.

19. Summers, C.M. Mathematical Expression of a Saturation Curve. G.E. Review. v 36 1933 p 182-185.

20. Thomson, W.T. Resonant Non-linear Control Circuits. Trans. AIEE. v 57 1938 p 469-476.

21. --------. The Generalized Solution for the Critical Conditions of the Ferro-resonant Parallel Circuit. Trans. AIEE v 58 1939 p 743-746.

22. ---------. Similitude of Critical Conditions in Ferro-resonant Circuits. Trans. AIEE v 58 1939 p 127-130.

23. Wilhelm, H. T. Measuring Inductance of Coils with Superimposed Direct Current. Bell Lab. Rec. v 14 1935 p 131-135.

24. Zenneck, J. Die Transformation eines Wechselstrome auf doppelte Wechselzahl mit Hülfe eines ruhenden Transformators. Ann. Phys. und Chemie. v 69 1899 p 858-860.

25. ---------. Contribution to the Theory of Magnetic Frequency Doublers. Proc. IRE. v 8 1920 p 468-492.

IX. ACKNOWLEDGEMENTS

The writer wishes to express his appreciation to Professor W. L. Cassell, for helpful suggestions and encouragement, to Professor B. S. Willis, for making available certain special laboratory equipment, and to Dr. W. B. Boast and other members of the staff of the Electrical Engineering Department for their suggestions and interest.

X. VITA

Author: John Douglas Ryder

Father's name: John Edwin Ryder

Mother's maiden name: Lucy May Rider

Date and place of birth: May 8, 1907, Columbus, Ohio.

Elementary and high schools attended:

Grandview Heights, Columbus, Ohio.

Universities attended:

The Ohio State University, Columbus, Ohio.

Case School of Applied Science, Cleveland, Ohio.

Iowa State College, Ames, Iowa

Degrees: Bachelor of Electrical Engineering, Ohio State University, 1928.

Master of Science, Ohio State University, 1929.

Field of Specialization: Electrical engineering, electronics and communications.

Professor in charge of major work: Prof. W. L. Cassell

Doctoral committee: Prof. W. L. Cassell

Dr. W. B. Boast

Dr. E. W. Anderson

Dr. L. T. Earls

XI. APPENDICES

Appendix A- Symbols

a	Constant of a steel
A	Area
B	Flux density
B_n	Constant of a steel
c	Constant of a steel
C	Capacity
D	$\frac{aAB_nN^2}{10^8 l}$
E	RMS voltage
e	Instantaneous voltage
E_m	Peak voltage
G	$\frac{E_m 10^8}{aB_nN}$
H	Magnetizing force
I	RMS current
i	Instantaneous current
k	Weighting constant
K	Galvanometer constant
K_1	Iron loss constant
K_2	Iron loss constant
L	Inductance
N	Number of turns
R	Resistance
R_c	Copper resistance of reactor
R_e	Effective resistance
R_k	Critical resistance
R_o	Constant resistance term
R	Circuit resistance less R_e
W	Watts
w	Weight
X	Reactance
Z	Impedance
α	aNi/l or aNI/l
α	Galvanometer deflection
$\mathcal{B}$	Intrinsic induction
ω	Angular frequency

Appendix B

The Gudermannian Function

X	gd X	x	gd X	x	gd x
0.00	0.000	2.00	1.302	4.00	1.534
0.10	0.100	2.10	1.327	4.20	1.541
0.20	0.199	2.20	1.350	4.40	1.546
0.30	0.296	2.30	1.371	4.60	1.551
0.40	0.390	2.40	1.390	4.80	1.554
0.50	0.480	2.50	1.407	5.00	1.557
0.60	0.567	2.60	1.423	5.20	1.560
0.70	0.649	2.70	1.437	5.40	1.562
0.80	0.726	2.80	1.449	5.60	1.563
0.90	0.798	2.90	1.461	5.80	1.565
1.00	0.866	3.00	1.471	6.00	1.566
1.10	0.928	3.10	1.481	∞	1.571
1.20	0.936	3.20	1.489		
1.30	1.039	3.30	1.497		
1.40	1.187	3.40	1.504		
1.50	1.132	3.50	1.510		
1.60	1.172	3.60	1.516		
1.70	1.209	3.70	1.521		
1.80	1.243	3.80	1.526		
1.90	1.274	3.90	1.530		